

Dependent Microstructure Noise and Integrated Volatility Estimation from High-Frequency Data

Z. Merrick Li*

Erasmus University Rotterdam

University of Amsterdam

and Tinbergen Institute

Roger J. A. Laeven†

Amsterdam School of Economics

University of Amsterdam, EURANDOM

and CentER

Michel H. Vellekoop‡

Amsterdam School of Economics

University of Amsterdam

March 11, 2022

Abstract

In this paper, we develop econometric tools to analyze the integrated volatility of the efficient price and the dynamic properties of microstructure noise in high-frequency data under general dependent noise. We first develop consistent estimators of the variance and autocovariances of noise using a variant of realized volatility. Next, we employ these estimators to adapt the pre-averaging method and derive a consistent estimator of the integrated volatility, which converges stably to a mixed Gaussian distribution at the optimal rate $n^{1/4}$. To refine the finite sample performance, we propose a two-step approach that corrects the finite sample bias, which turns out to be crucial in applications. Our extensive simulation studies demonstrate the excellent performance of our two-step estimators. In an empirical study, we characterize the dependence structures of microstructure noise in several popular sampling schemes and provide intuitive economic interpretations; we also illustrate the importance of accounting for both the serial dependence in noise and the finite sample bias when estimating integrated volatility.

Keywords: Dependent microstructure noise, realized volatility, bias correction, pre-averaging method, strongly mixing sequences.

JEL classification: C13, C14, C55, C58.

*Corresponding author. University of Amsterdam, Amsterdam School of Economics, PO Box 15867, 1001 NJ Amsterdam, The Netherlands. Email: Z.Merrick.Li@gmail.com. Phone: +31 (0)20 5254252.

†University of Amsterdam, Amsterdam School of Economics, PO Box 15867, 1001 NJ Amsterdam, The Netherlands. Email: R.J.A.Laeven@uva.nl. Phone: +31 (0)20 5254219.

‡University of Amsterdam, Amsterdam School of Economics, PO Box 15867, 1001 NJ Amsterdam, The Netherlands. Email: M.H.Vellekoop@uva.nl. Phone: +31 (0)20 5254210.

1 Introduction

Over the past decade and a half, high-frequency financial data have become increasingly available. In tandem, the development of econometric tools to study the dynamic properties of high-frequency data has become an important subject area in economics and statistics. A major challenge is provided by the accumulation of market microstructure noise at higher frequencies, which can be attributed to various market microstructure effects including, for example, information asymmetries (see [Glosten and Milgrom \(1985\)](#)), inventory controls (see [Ho and Stoll \(1981\)](#)), discreteness of the data (see [Harris \(1990\)](#)), and transaction costs (see [Garman \(1976\)](#)).

It has been well-established (see, e.g., [Black \(1986\)](#)) that the observed transaction price¹ Y can be decomposed into the unobservable “efficient price” (or “frictionless equilibrium price”) X plus a noise component U that captures market microstructure effects. That is, it is natural to assume that

$$Y_t = X_t + U_t, \tag{1}$$

where further assumptions on X and U need to be stipulated. While estimating the integrated volatility of the efficient price is the emblematic problem in high-frequency financial econometrics (see, for example, [Aït-Sahalia and Jacod \(2014\)](#)), the study of microstructure noise, e.g., its magnitude, dynamic properties, etc., is the main focus of the market microstructure literature (see, for example, [Hasbrouck \(2007\)](#)). A common challenge, however, is that the two components of the observed price Y in (1) are latent. Therefore, distributional features of one component, say, of the microstructure noise, will affect the estimation of characteristics of the other, such as the integrated volatility of the efficient price.²

While the semimartingale framework provides the natural class to model the efficient price (see, e.g., [Duffie \(2010\)](#)), the statistical assumptions on noise induced by microeconomic financial models range from simple to very complex, depending on which phenomena the model aims to capture. For example, the classic Roll model (see [Roll \(1984\)](#)) postulates an i.i.d. bid-ask bounce resulting from uncorrelated order flows; [Hasbrouck and Ho \(1987\)](#), [Choi et al. \(1988\)](#), and [Stoll \(1989\)](#) introduce autocorrelated order flows, yielding autoregressive microstructure noise; and [Gross-Kluschmann and Hautsch \(2013\)](#) model microstructure noise with long-memory properties. Therefore, being able to account for the potentially complex statistical behavior of microstructure noise that contaminates our observations of the semimartingale efficient price dynamics, would be an appealing property of any method that aims at disentangling the efficient price and microstructure noise.

¹In this paper, “price” always refers to the “logarithmic price”.

²Indeed, while high-frequency data in principle facilitate the asymptotic and empirical analysis of volatility estimators, the pronounced presence of microstructure noise at high frequency subverts the desirable properties of traditional estimators such as realized volatility.

To estimate the integrated volatility of the efficient price, several de-noise methods have been developed, mostly assuming i.i.d. microstructure noise. Examples include the two-scale and multi-scale realized volatility estimators developed in [Zhang et al. \(2005\)](#) and [Zhang \(2006\)](#), the realized kernel methods developed in [Barndorff-Nielsen et al. \(2008\)](#), the likelihood approach initiated by [Aït-Sahalia et al. \(2005\)](#) and [Xiu \(2010\)](#), and the pre-averaging method developed in a series of papers by [Podolskij and Vetter \(2009b\)](#) and [Jacod et al. \(2009, 2010\)](#), see also [Podolskij and Vetter \(2009a\)](#). The variance of noise is usually obtained as a by-product.

In this paper, we allow the microstructure noise to be serially dependent in a general setting, nesting many special cases (including independence). We do not impose any parametric restrictions on the distribution of the noise, except for some rather general mixing conditions that guarantee the existence of limit distributions, hence our approach is essentially nonparametric. In this setting, we first derive the stochastic limit of the realized volatility of observed prices after j lags. Using this limit result, we develop consistent estimators of the variance and covariances of noise. The aim of estimating the second moments of noise is twofold. On the one hand, we would like to explore the dynamic properties of microstructure noise. In particular, we would like to compare these properties to those induced by various parametric models of microstructure noise based on leading microstructure theory, and obtain corresponding economic interpretations to achieve a better understanding of the microstructure effects in high-frequency data. On the other hand, the second moments of noise become nuisance parameters in estimating the integrated volatility, which is a prime objective in the analysis of high-frequency financial data.

To estimate the integrated volatility, we next adapt the pre-averaging estimator (PAV) to allow for serially dependent noise in our general setting. We find that the stochastic limit of the adapted PAV estimator is a function of the volatility and the variance and covariances of noise, and the latter, constituting an *asymptotic bias*, can be consistently estimated by our realized volatility estimator. Hence, we can correct the asymptotic bias, resulting in centered estimators of the integrated volatility.

A key interest in this paper is to unravel the interplay between asymptotic and finite sample biases when estimating integrated volatility. In a finite sample analysis, we find that the realized volatility estimator has a finite sample bias that is proportional to the integrated volatility. The bias term becomes significant when the number of lags (in computing the variant of realized volatility) is large, or the noise-to-signal ratio³ is small. Therefore, we are in a situation in which the integrated volatility generates a *finite sample bias* to the estimators of the second moments of noise, while the latter become the *asymptotic bias* in estimating the former. This “feedback effect” in the bias corrections motivates us to develop *two-step estimators*. First, we simply ignore the dependence in noise and proceed with the

³The ratio of the variance of noise and the integrated volatility.

pre-averaging method to obtain an estimator of the integrated volatility. Next, we use this estimator to obtain *finite sample bias* corrected estimators of the second moments of noise, which can then be used to correct the asymptotic bias yielding the second-step estimator of the integrated volatility. Repeating this process leads to three-step estimators (and beyond) which may further improve the two-step estimators on average, but at the cost of higher standard deviations. Figure 1 gives a simple graphical illustration of the implementation of the two-step estimators.

We conduct extensive Monte Carlo experiments to examine the performance of our estimators, which proves to be excellent. We demonstrate in particular that they can accommodate both serially dependent and independent noise and perform well in finite samples with realistic data frequencies and sample sizes. The experiments reveal the importance of a unified treatment of asymptotic and finite sample biases when estimating integrated volatility.

Empirically, we apply our new estimators to a sample of Citigroup transaction data. We find that the associated microstructure noise tends to be positively autocorrelated. This is in line with earlier findings in the microstructure literature, see [Hasbrouck and Ho \(1987\)](#), [Choi et al. \(1988\)](#), and [Huang and Stoll \(1997\)](#). Attributing this positive autocorrelation to order flow continuation, the estimated probability that a buy (or sell) order follows another buy (or sell) order is 0.87. Furthermore, microstructure noise turns out to be negatively autocorrelated under tick time sampling. This is consistent with inventory models, in which dealers alternate quotes to maintain their inventory position. We obtain an estimate of the probability of reversed orders equal to 0.84. Turning to the estimators of integrated volatility, we find that with positively autocorrelated noise the commonly adopted methods that hinge on the i.i.d. assumption of noise tend to overestimate the integrated volatility. Under two alternative (sub)sampling schemes — regular time sampling and tick time sampling — our estimators also appear to work well. This testifies to the critical relevance of the bias corrections embedded in our two-step estimators.

In earlier literature, [Aït-Sahalia et al. \(2011\)](#) show that the two-scale and multi-scale realized volatility estimators are robust to exponentially decaying dependent noise. In this paper, we provide explicit estimators of the second moments of noise and analyze their asymptotic behavior, develop bias-corrected estimators of the integrated volatility based on these moments of noise, and empirically assess the noise characteristics under different sampling schemes. Furthermore, [Hautsch and Podolskij \(2013\)](#) study q -dependent microstructure noise, develop consistent estimators of the first q autocovariances of microstructure noise and define the associated pre-averaging estimators. An appealing feature of their approach is that their autocovariance-type estimators of q -dependent noise consider non-overlapping increments which avoids finite sample bias. We allow for more general assumptions on the dependence structure of microstructure noise. Owing to its generality our setting incorporates many microstructure models as special cases. We therefore do not need to advocate any particular model of microstructure

noise and this enables us to obtain economic interpretations of our empirical results under multiple sampling schemes.

In two contemporaneous and independent works, [Jacod et al. \(2017a,b\)](#) also study dependent noise in high-frequency data. In [Jacod et al. \(2017b\)](#), they develop a novel local averaging method to “recover” the noise and they can, in principle, estimate any finite (joint) moments of noise with diurnal features. Moreover, they also allow observation times to be random. Empirically, they find some interesting statistical properties of noise. In particular, they find that noise is strongly serially dependent with polynomially decaying autocorrelations. Employing this local averaging method, [Jacod et al. \(2017a\)](#) develop an estimator of integrated volatility that allows for dependent noise. To distinguish our work from these two papers, we first note that our assumptions on noise are slightly different: we assume that the noise process constitutes a strongly mixing sequence while they require a ρ -mixing sequence (see [Bradley \(2005\)](#) for a discussion of mixing sequences). Furthermore, the local averaging method differs from, and allows to analyze more general noise characteristics than, the simpler realized volatility method developed here. The key difference is our explicit treatment of the feedback effect between the asymptotic and finite sample biases: we show that in a finite sample, the integrated volatility and second moments of microstructure noise should be estimated in a unified way, since they induce biases in each other. We design novel and easily implementable two-step estimators to correct for the intricate biases. Our two-step estimators of the integrated volatility, which are designed to allow for dependent noise, also perform well in the special case of independent noise, and in a sample of reasonable size as encountered in practice. This robustness to (mis)specification of noise and to sampling frequencies is an important advantage of our two-step estimators. Our unified treatment of the asymptotic and finite sample biases may help explain why the empirical studies in [Jacod et al. \(2017b\)](#) render the strong dependence in noise they find (and question themselves); see our empirical analysis in [Section 7](#).

In another independent paper, [Da and Xiu \(2017\)](#) introduce a novel quasi maximum likelihood approach to estimate both the volatility and the autocovariances of moving-average microstructure noise. They also extend their estimators to general settings that allow for irregular observation times, intraday patterns of noise and jumps in asset prices. Their approach treats “large” and “small” microstructure noise in a uniform way which leads to a potential improvement in the convergence rate. Our approach is essentially of a nonparametric nature and provides unified estimators of a class of volatility functionals (see [Theorem 4.1](#)) including the asymptotic variance, which account for the feedback between finite sample and asymptotic biases. Our empirical study also has a different focus. Our investigation is not as extensive as in [Da and Xiu \(2017\)](#),⁴ but we explicitly consider different sampling schemes,⁵ analyzing

⁴Da and Xiu maintain a website to provide up-to-date daily annualized volatility estimates for all S&P 1500 index constituents, see <http://dachxiu.chicagobooth.edu/#risklab>.

⁵In their empirical studies, [Da and Xiu \(2017\)](#) only consider tick time sampling.

the autocovariance patterns of noise in connection to microstructure noise models and their impact on integrated volatility estimation.

The remainder of this paper is organized as follows. In Section 2, we introduce the basic setting and notation. In Section 3, we analyze realized volatility with dependent noise and develop consistent estimators of the second moments of noise. The pre-averaging method with dependent noise is studied in Section 4. Section 5 introduces our two-step estimators. Section 6 reports extensive simulation studies. Our empirical study is presented in Section 7. Section 8 concludes the paper. All proofs and some additional Monte Carlo simulation and empirical results are collected in an online appendix, see [Li et al. \(2018\)](#).

2 Framework and Assumptions

We assume that the efficient log-price process X is represented by a continuous Itô semimartingale defined on a filtered probability space $(\Omega, \mathcal{F}, (\mathcal{F}_t)_{t \geq 0}, \mathbb{P})$:

$$X_t = X_0 + \int_0^t a_s ds + \int_0^t \sigma_s dW_s, \quad (2)$$

where W is a standard Brownian motion, the drift process a_s is optional and locally bounded, and the volatility process σ_s is adapted with càdlàg paths. The probability space also supports the noise process U . We assume that all observations are collected in the fixed time interval $[0, T]$, where without losing generality we let $T = 1$. At stage n , the observation times are given by $0 = t_0^n < t_1^n < \dots < t_n^n = 1$.

Assumption 2.1 (Market microstructure noise). *The noise process $(U_i)_{i \in \mathbb{N}}$ satisfies the following assumptions:*

1. U is symmetrically distributed around 0;
2. The noise process U is independent of the efficient log-price process X ;
3. U is stationary and strongly mixing and the mixing coefficients⁶ $\{\alpha_h\}_{h=1}^\infty$ decay at a polynomial rate, i.e., there exist some constants $C > 0, v > 0$ such that

$$\alpha_h \leq \frac{C}{h^v}. \quad (3)$$

Moreover, we assume U has bounded moments of all orders.

⁶The mixing coefficients constitute a sequence satisfying

$$|\mathbb{P}(A \cap B) - \mathbb{P}(A)\mathbb{P}(B)| \leq \alpha_h,$$

for all $A \in \sigma(U_0, \dots, U_k), B \in \sigma(U_{k+h}, U_{k+h+1}, \dots)$, where $\sigma(A)$ is the σ -algebra generated by A . We refer to [Bradley \(2007\)](#) or Chapter VIII of [Jacod and Shiryaev \(2003\)](#) for further details on and properties of mixing sequences.

The mixing conditions in Assumption 2.1 item (3.) ensure that the noise process evaluated at different time instances, say, $i, i+h$, is increasingly limited in dependence when the lag h increases. In particular, there exists some $C' > 0$ such that

$$|\gamma(h)| \leq \frac{C'}{h^{v/2}}, \quad (4)$$

where $\gamma(h) = \mathbf{Cov}(U_i, U_{i+h})$ is the autocovariance function of U . Assuming U to have bounded moments of all orders is not strictly necessary. Depending on the targeted moments, this assumption can be relaxed via the choice of v in (3), see Lemma VIII 3.102 in Jacod and Shiryaev (2003). Throughout the paper we maintain the assumption of bounded moments of all orders and only specify the restrictions on v .

At stage n , we will denote U_i by U_i^n , $\forall i \leq n$. The i -th observed price is thus given by

$$Y_i^n = X_i^n + U_i^n, \quad (5)$$

where $X_i^n = X_{t_i^n}$. In the remainder of the main text, we assume $t_i^n = i/n, i = 0, \dots, n$; see Appendix F for an analysis of irregular sampling schemes.

Remark 2.1 (Microstructure noise and sampling schemes). *We allow the noise process U to generate dependencies in sampling time, including transaction time,⁷ calendar time,⁸ and tick time.⁹ Hence, our noise process essentially constitutes a discrete-time model — it does not depend explicitly on the time between successive observations. Aït-Sahalia et al. (2005), Hansen and Lunde (2006), and Hansen et al. (2008) study various continuous-time models of dependent microstructure noise. In these continuous-time models, the noise component of a log-return over a time interval Δ is of order $O_p(\sqrt{\Delta})$, the same order as the logarithmic return of the efficient price.*

Remark 2.2 (General dynamic properties of microstructure noise). *Our assumptions on the dependence of noise are quite general, nesting many models as special cases including, for example, i.i.d. noise, q -dependent noise (under which $\gamma(h) = 0, \forall h > q$), ARMA(p, q) noise (see Mokkadem (1988)) and some long-memory processes (see Tsay (2005)). We note that AR(1) and AR(2) noise are studied in Barndorff-Nielsen et al. (2008) and Hendershott et al. (2013) respectively, q -dependent noise is considered by Hansen et al. (2008) and Hautsch and Podolskij (2013), while Gross-Kluschmann and Hautsch (2013) study long-memory bid-ask spreads.*

⁷Under this sampling scheme, Y_i^n (resp. X_i^n, U_i^n) is the observed log-price (resp. efficient log-price, microstructure noise) associated with the i -th trade. The observation times $(t_i^n)_{0 \leq i \leq n}$ can, in general, be deterministic or random, and regular or irregular.

⁸Under this sampling scheme, Y_i^n (resp. X_i^n, U_i^n) is the observed log-price (resp. efficient log-price, microstructure noise) at regular time $i\Delta_n$, with $\Delta_n = 1/n$ in the main text.

⁹Tick time sampling removes all zero returns; see Aït-Sahalia et al. (2011) and Griffin and Oomen (2008). Hence, Y_i^n is by definition different from Y_{i-1}^n and Y_{i+1}^n under this sampling scheme.

3 Estimation of the Variance and Covariances of Noise

In this section, we develop consistent estimators of the second moments of noise under Assumption 2.1. These estimators will later serve as important inputs to adapt the pre-averaging method. We also analyze our estimators' finite sample properties.

3.1 Realized volatility with dependent noise

We start with the following preliminary result:

Proposition 3.1. *Assume that the efficient log-price follows (2), the observations follow (5), and the noise process satisfies Assumption 2.1. Furthermore, let j be a fixed integer and assume the sequence j_n and the exponent v satisfy the following conditions:*

$$v > 2, \quad j_n \rightarrow \infty, \quad j_n/n \rightarrow 0. \quad (6)$$

Then we have the following convergences in probability as $n \rightarrow \infty$:

$$\widehat{\langle Y, Y \rangle}_n(j) := \frac{\sum_{i=0}^{n-j} (Y_{i+j}^n - Y_i^n)^2}{2(n-j+1)} \xrightarrow{\mathbb{P}} \mathbf{Var}(U) - \gamma(j), \quad (7)$$

$$\widehat{\mathbf{Var}(U)}_n := \frac{\sum_{i=0}^{n-j_n} (Y_{i+j_n}^n - Y_i^n)^2}{2(n-j_n+1)} \xrightarrow{\mathbb{P}} \mathbf{Var}(U), \quad (8)$$

$$\widehat{\gamma(j)}_n := \widehat{\mathbf{Var}(U)}_n - \widehat{\langle Y, Y \rangle}_n(j) \xrightarrow{\mathbb{P}} \gamma(j). \quad (9)$$

Proof. See Appendix A. □

The special case of (7) that occurs when $j = 1$ appears in Aït-Sahalia et al. (2011) assuming exponential decay. We also note that in the most recent version of Jacod et al. (2017b) similar estimators as $\widehat{\langle Y, Y \rangle}_n(j)$ are mentioned but without formal analysis of their limiting behavior. To our best knowledge, our paper is the first to estimate the variance and covariances of noise using realized volatility under a general dependent noise setting.

3.2 Finite sample bias correction

The theoretical validity of our realized volatility estimators in (7)–(9) hinges on the increasing availability of observations in a fixed time interval, the so-called *infill asymptotics*. In general, an estimator derived from asymptotic results can, however, behave very differently in finite samples. Our realized volatility

estimators of the second moments of noise are an example for which the asymptotic theory provides a poor representation of the estimators' finite sample behavior.¹⁰

Intuitively, the finite sample bias stems from the diffusion component, when computing the realized volatility $\widehat{\langle Y, Y \rangle}_n(j)$ over large lags j in a finite sample, and we will explain later (e.g., in Remark 3.3) why it is critically relevant to account for it in real applications. In the sequel, we assume the drift a_t in (2) to be zero. According to, for example, Bandi and Russell (2008) and Lee and Mykland (2012) this is not restrictive in high-frequency analysis. This will be confirmed in our Monte Carlo simulation studies in Section 6 and Appendix H.

Proposition 3.2. *Assume that the efficient log-price follows (2) with $a_s = 0 \forall s$, and assume there is some $\delta > 0$ so that σ_t is bounded for all $t \in [0, \delta] \cup [1 - \delta, 1]$. Furthermore, assume the observations follow (5), and the noise process satisfies Assumption 2.1. Then, conditional on the volatility path,*

$$\mathbb{E}_\sigma \left(\widehat{\langle Y, Y \rangle}_n(j) \right) = \frac{j \int_0^1 \sigma_t^2 dt}{2(n-j+1)} + \mathbf{Var}(U) - \gamma(j) + O_p(j^2/n^2). \quad (10)$$

Here, $\mathbb{E}_\sigma(\cdot)$ is the expectation conditional on the entire path of volatility.

Proof. See Appendix B. □

Remark 3.1. *The regularity conditions with respect to σ_t in Proposition 3.2 trivially hold if the volatility is assumed to be continuous. (Volatility is usually assumed to be continuous when making finite sample bias corrections.)*

Remark 3.2. *Let $j = 1$ and let us restrict attention to sampling in calendar time. In that special case the result in Proposition 3.2 bears similarities with Theorem 1 in Hansen and Lunde (2006). Contrary to Hansen and Lunde (2006) we assume that the efficient log-price X is independent of the noise U . Therefore, any correlations between the two drop out.*

Proposition 3.2 reveals that $\widehat{\langle Y, Y \rangle}_n(j) - \frac{j \int_0^1 \sigma_t^2 dt}{2(n-j+1)}$ will be a better estimator of $\mathbf{Var}(U) - \gamma(j)$ in finite samples, and it motivates the following finite sample bias corrected estimators:

$$\widehat{\langle Y, Y \rangle}_n^{(\text{adj})}(j) := \widehat{\langle Y, Y \rangle}_n(j) - \frac{\hat{\sigma}^2 j}{2(n-j+1)}; \quad (11)$$

$$\widehat{\mathbf{Var}(U)}_n^{(\text{adj})} := \widehat{\mathbf{Var}(U)}_n - \frac{\hat{\sigma}^2 j_n}{2(n-j_n+1)}; \quad (12)$$

$$\widehat{\gamma(j)}_n^{(\text{adj})} := \widehat{\mathbf{Var}(U)}_n^{(\text{adj})} - \widehat{\langle Y, Y \rangle}_n^{(\text{adj})}(j); \quad (13)$$

¹⁰This applies to the local averaging estimators developed in Jacod et al. (2017b) as well; see Footnote 11 for further details.

where $\hat{\sigma}^2$ is an estimator of $\int_0^1 \sigma_s^2 ds$. We note that the bias corrected estimators are still consistent, as the fraction $\frac{j}{n-j+1}$ is negligible when j is much smaller than n .

Remark 3.3 (Why the finite sample bias matters). *We now explain why the finite sample bias correction is crucial in applications. We first rewrite (10):*

$$\begin{aligned}\mathbb{E}_\sigma\left(\widehat{\langle Y, Y \rangle}_n(j)\right) &= \frac{j \int_0^1 \sigma_t^2 dt}{2(n-j+1)} + \mathbf{Var}(U) - \gamma(j) + O_p(j^2/n^2) \\ &= (\mathbf{Var}(U) - \gamma(j)) \left(1 + \frac{\frac{j}{2(n-j+1)}}{\frac{\mathbf{Var}(U) - \gamma(j)}{\int_0^1 \sigma_t^2 dt}}\right) + O_p(j^2/n^2).\end{aligned}\tag{14}$$

Observe that the finite sample bias is determined by the ratio of the two terms $\frac{j}{2(n-j+1)}$ and $\frac{\mathbf{Var}(U) - \gamma(j)}{\int_0^1 \sigma_t^2 dt}$. The first term, $\frac{j}{2(n-j+1)}$, depends on the data frequency (n) and “target parameters” (j); the second term, $\frac{\mathbf{Var}(U) - \gamma(j)}{\int_0^1 \sigma_t^2 dt}$, is the (latent) noise-to-signal ratio. If the second term is “relatively larger (smaller)” than the first one, then the finite sample bias will be small (large). In other words, the finite sample bias is not only determined by the data frequency and target parameters, but also by other properties of the underlying efficient price and noise processes.

In high-frequency financial data, the noise-to-signal ratio $\frac{\mathbf{Var}(U)}{\int_0^1 \sigma_t^2 dt}$ is typically small, but it can vary from $O(10^{-2})$ (see [Bandi and Russell \(2006\)](#)) to $O(10^{-6})$ (see [Christensen et al. \(2014\)](#)) in empirical studies. The ratio $\frac{j}{2(n-j+1)}$, while typically small as well, can still be relatively large, depending on the specific situation. Consider the following two scenarios:

- 1) We have ultra high-frequency data with $n = O(10^5)$ (recall that the number of seconds in a business day is 23,400), and we select $j_n = 20$. Then, the ratio $\frac{j_n}{2(n-j_n+1)} = O(10^{-4})$.
- 2) We have i.i.d. noise and we would like to estimate the variance of noise by $\widehat{\langle Y, Y \rangle}_n(1)$ using high-frequency data with average duration of 20 seconds (thus $n \approx 10^3$); see, e.g., [Bandi and Russell \(2006\)](#). Hence, $\frac{j}{2(n-j+1)} = O(10^{-3})$.

In both scenarios, the ratio of $\frac{j}{2(n-j+1)}$ and $\frac{\mathbf{Var}(U) - \gamma(j)}{\int_0^1 \sigma_t^2 dt}$ can vary widely, depending on the magnitude of the latent noise-to-signal ratio. It is then clear from the first line of (14) that the finite sample bias term, which is proportional to the integrated volatility, may well wipe out the variance of noise, depending on the specific situation.

Remark 3.4. Note that increasing the sample size by extending the time horizon to $[0, T]$ with large T will not remove the finite sample bias. Hence, the finite sample bias may be viewed as a low frequency bias.

4 The Pre-Averaging Method with Dependent Noise

In this section, we adapt a popular “de-noise” method — the pre-averaging method — to allow for serially dependent noise in our general setting. The pre-averaging method was originally introduced by Podolskij and Vetter (2009b) (see also Jacod et al. (2009), Jacod et al. (2010), Podolskij and Vetter (2009a), and Hautsch and Podolskij (2013)).

4.1 Setup and notation

For a generic process V , we denote its pre-averaged version by

$$\bar{V}_m^n := \frac{1}{k_n + 1} \sum_{i=(2m-2)k_n}^{(2m-1)k_n} (V_{i+k_n}^n - V_i^n), \quad (15)$$

for $1 \leq m \leq M_n$ with $M_n = \lfloor \frac{\sqrt{n}}{2c} \rfloor$, where $k_n \in \mathbb{N}$ satisfies

$$k_n = c\sqrt{n} + o(n^{1/4}), \quad (16)$$

for some positive constant c and where $\lfloor \cdot \rfloor$ is the floor function. For any real $r \geq 2$, the pre-averaged statistics of the log-price process Y are defined as follows:

$$\text{PAV}(Y, r)_n := n^{\frac{r-2}{4}} \sum_{m=1}^{M_n} |\bar{Y}_m^n|^r, \quad r \geq 2. \quad (17)$$

Remark 4.1. Equation (15) invokes a simple version of the pre-averaging method. In particular, we take a simple weighting function to compute the pre-averages in the m -th non-overlapping interval. We refer to Jacod et al. (2009, 2010) and Podolskij and Vetter (2009a) for the pre-averaging method with general weighting functions and pre-averaged values based on overlapping intervals.

We first present the following proposition, which provides the asymptotic distribution of the pre-averaged noise:

Proposition 4.1. Assume that the noise satisfies Assumption 2.1 with $v > 2$ and that σ_U^2 defined below is strictly positive. Then, the following central limit theorem holds for \bar{U}_m^n :

$$n^{1/4} \bar{U}_m^n \xrightarrow{\mathcal{L}} \mathcal{N}\left(0, \frac{2\sigma_U^2}{c}\right), \quad (18)$$

where

$$\sigma_U^2 = \mathbf{Var}(U) + 2 \sum_{j=1}^{\infty} \gamma(j), \quad (19)$$

and c is defined in (16).

Proof. See Appendix C. □

For i.i.d. noise, σ_U^2 reduces to $\mathbf{Var}(U)$, and it is known (see Zhang et al. (2005) and Bandi and Russell (2008)) that the variance of noise can be consistently estimated by the standardized realized volatility of observed returns. However, when noise is dependent we face a much more complex situation: all variance and covariance terms constitute σ_U^2 . Nevertheless, we can provide a consistent estimator of σ_U^2 , as follows:

Proposition 4.2. *Let $v > 2$ and $j_n^3/n \rightarrow 0$. Define*

$$\widehat{\sigma_U^2} := \widehat{\mathbf{Var}(U)}_n + 2 \sum_{j=1}^{i_n} \widehat{\gamma(j)}_n, \quad (20)$$

where i_n satisfies the conditions $i_n \rightarrow \infty, i_n \leq j_n$, and $\widehat{\mathbf{Var}(U)}_n$ and $\widehat{\gamma(j)}_n$ are defined in (8) and (9). Then,

$$\widehat{\sigma_U^2} \xrightarrow{\mathbb{P}} \sigma_U^2. \quad (21)$$

Proof. See Appendix D. □

4.2 Asymptotic theory: Consistency

The following results establish consistency and a central limit theorem for the pre-averaged log-price process under dependent noise in our general setting.

Theorem 4.1. *Assume that the efficient log-price follows (2), the observations follow (5), and the noise process satisfies Assumption 2.1. Then, for any even integer $r \geq 2$,*

$$\text{PAV}(Y, r)_n \xrightarrow{\mathbb{P}} \text{PAV}(Y, r) := \frac{\mu_r}{2c} \int_0^1 \left(\frac{2c}{3} \sigma_s^2 + \frac{2}{c} \sigma_U^2 \right)^{\frac{r}{2}} ds, \quad (22)$$

where σ_U^2 is defined in (19) and $\mu_r = \mathbb{E}(Z^r)$ for a standard normal random variable Z .

Proof. See Appendix E. □

Corollary 4.1. *Under the assumptions of Proposition 4.2 and Theorem 4.1, we have the following consistency result for the integrated volatility:*

$$\widehat{\text{IV}}_n := 3 \left(\text{PAV}(Y, 2)_n - \frac{\widehat{\sigma_U^2}}{c^2} \right) \xrightarrow{\mathbb{P}} \int_0^1 \sigma_s^2 ds, \quad (23)$$

where $\widehat{\sigma_U^2}$ is defined in (20).

4.3 Asymptotic theory: The central limit theorem

Theorem 4.2. *Assume that the efficient log-price follows (2), the observations follow (5), and the noise process satisfies Assumption 2.1. Furthermore, assume that the process σ is a continuous Itô semimartingale, and the assumptions of Proposition 4.2 hold with $v > 4$. Then,*

$$n^{1/4} \left(\widehat{\text{IV}}_n - \int_0^1 \sigma_s^2 ds \right) \xrightarrow{\mathcal{L}^{-s}} \int_0^1 \left(2\sqrt{c}\sigma_s^2 + \frac{6\sigma_U^2}{c^{3/2}} \right) dW'_s, \quad (24)$$

where $\xrightarrow{\mathcal{L}^{-s}}$ denotes stable convergence in law and where W' is a standard Wiener process independent of \mathcal{F} . Moreover, letting $\tau_n^2 := 6\text{PAV}(Y, 4)_n$, we have that

$$\frac{n^{1/4} \left(\widehat{\text{IV}}_n - \int_0^1 \sigma_s^2 ds \right)}{\tau_n} \quad (25)$$

converges stably in law to a standard normal random variable, which is independent of \mathcal{F} .

Proof. See Appendix G. □

Remark 4.2. *The limit result in (24) provides a simple rule to select c conditional on the volatility path: c can be chosen to minimize the asymptotic variance. The optimal c thus obtained is given by*

$$c^* = 3 \sqrt{\frac{\sigma_U^2}{\int_0^1 \sigma_s^2 ds}}. \quad (26)$$

This result is intuitive: if the noise-to-signal ratio is large, we should pick a large c , hence include more observations in a local pre-averaging window to reduce the noise effect. With typical noise-to-signal ratios that range from 10^{-2} to 10^{-4} as encountered in practice, the optimal $c^ \in [0.03, 0.3]$. In our simulation and empirical studies, we throughout fix $c = 0.2$.*

5 Two-Step Estimators and Beyond

In this section, we present our two-step estimators of the integrated volatility and the second moments of noise based on both our asymptotic theory and finite sample analysis.

We observe from Corollary 4.1 that the second moments of noise contribute to an *asymptotic bias* in the estimation of the integrated volatility. But our finite sample analysis indicates that we need an estimator of the integrated volatility to correct the *finite sample bias* when estimating the second moments of noise. Our two-step estimators are specifically designed for the purpose of correcting the “interlocked” bias.

In the first step, we ignore the dependence in noise and estimate the variance of noise by realized volatility. Hence, our first-step estimators of the second moments of noise are given by

$$\widehat{\mathbf{Var}}(U)_{\text{step1}} := \widehat{\langle Y, Y \rangle}_n(1); \quad \widehat{\gamma(j)}_{\text{step1}} := 0; \quad \widehat{\sigma}_{U, \text{step1}}^2 := \widehat{\langle Y, Y \rangle}_n(1). \quad (27)$$

Next, we proceed with the pre-averaging method to obtain the first-step estimator of the integrated volatility:

$$\widehat{\mathbf{IV}}_{\text{step1}} := 3 \left(\text{PAV}(Y, 2)_n - \frac{\widehat{\sigma}_{U, \text{step1}}^2}{c^2} \right). \quad (28)$$

To initiate the second step, we first replace $\hat{\sigma}^2$ by $\widehat{\mathbf{IV}}_{\text{step1}}$ in (11) and (12) and obtain the second-step estimators of the variance and covariances of noise as follows:

$$\widehat{\langle Y, Y \rangle}_{\text{step2}}(j) := \widehat{\langle Y, Y \rangle}_n(j) - \frac{j \widehat{\mathbf{IV}}_{\text{step1}}}{2(n-j+1)}; \quad (29)$$

$$\widehat{\mathbf{Var}}(U)_{\text{step2}} := \widehat{\mathbf{Var}}(U)_n - \frac{j_n \widehat{\mathbf{IV}}_{\text{step1}}}{2(n-j_n+1)}; \quad (30)$$

$$\widehat{\gamma(j)}_{\text{step2}} := \widehat{\mathbf{Var}}(U)_{\text{step2}} - \widehat{\langle Y, Y \rangle}_{\text{step2}}(j); \quad (31)$$

$$\widehat{\sigma}_{U, \text{step2}}^2 := \widehat{\mathbf{Var}}(U)_{\text{step2}} + 2 \sum_{j=1}^{i_n} \widehat{\gamma(j)}_{\text{step2}}. \quad (32)$$

Then, the second-step estimator of the integrated volatility is given by

$$\widehat{\mathbf{IV}}_{\text{step2}} := 3 \left(\text{PAV}(Y, 2)_n - \frac{\widehat{\sigma}_{U, \text{step2}}^2}{c^2} \right). \quad (33)$$

The asymptotic properties of the two-step estimators are inherited from the asymptotic properties derived in the previous section. Of course, one can iterate beyond the two steps to obtain k -step estimators, for example, $\widehat{\mathbf{IV}}_{\text{step3}}$. The next section will present simulation evidence to compare the performances of the proposed estimators. As the results in the following section reveal, the two-step

estimators already perform very well.

6 Simulation Study

6.1 Simulation design

We consider an autoregressive noise process U given by the following dynamics:

$$U_t = V_t + \epsilon_t, \quad (34)$$

where V is centered i.i.d. Gaussian and ϵ is an AR(1) process with first-order coefficient ρ , $|\rho| < 1$. The processes V and ϵ are assumed to be statistically independent. As benchmark parameters, we use the GMM estimates of the noise parameters from [Aït-Sahalia et al. \(2011\)](#) given by $\mathbb{E}(V^2) = 2.9 \times 10^{-8}$, $\mathbb{E}(\epsilon^2) = 4.3 \times 10^{-8}$, and $\rho = -0.7$. We also allow for different dependence structures by varying our choice of ρ . Furthermore, the efficient log-price X is assumed to follow an Ornstein-Uhlenbeck process:

$$dX_t = -\delta(X_t - \mu)dt + \sigma dW_t, \quad \delta > 0, \sigma > 0. \quad (35)$$

We set $\sigma^2 = 6 \times 10^{-5}$, $\delta = 0.5$, and $\mu = 1.6$, and assume the processes X and U to be mutually independent. The signal-to-noise ratio induced by this model for $Y_t = X_t + U_t$ is realistic, according to empirical studies; see, e.g., [Bandi and Russell \(2006, 2008\)](#). For all the experiments in this section, we conduct 1,000 simulations. Each simulated sample consists of 23,400 observations in our fixed time interval $[0, 1]$ representing one trading day of data sampled at the 1-sec time scale with 6.5 trading hours per day. The ultra high-frequency case with sampling at the 0.05-sec time scale is also considered. We take $c = 0.2$.

6.2 Realized volatility estimators of the second moments of noise

To get a first impression of the properties of our estimator $\widehat{\langle Y, Y \rangle}_n(j)$ defined in (7), we plot $\widehat{\langle Y, Y \rangle}_n(j)$ against the number of lags j in Figure 2. In addition to $\widehat{\langle Y, Y \rangle}_n(j)$, we also plot the bias adjusted version $\widehat{\langle Y, Y \rangle}_n^{(\text{adj})}(j)$ defined in (11), in which we employ three “approximations” to the integrated volatility that $\widehat{\langle Y, Y \rangle}_n^{(\text{adj})}(j)$ depends on: $\hat{\sigma}_H^2 = 1.2\sigma^2$, $\hat{\sigma}_M^2 = \sigma^2$, and $\hat{\sigma}_L^2 = 0.8\sigma^2$. Figure 2 shows that a prominent feature of our realized volatility estimator $\widehat{\langle Y, Y \rangle}_n(j)$ is that it deviates from its stochastic limit $\text{Var}(U) - \gamma(j)$ almost linearly in the number of lags j , as predicted by Proposition 3.2. The deviation, induced by the finite sample bias, can be corrected to a large extent when only rough “estimates” of the integrated volatility are available. In the ideal but infeasible situation that we know the true volatility

($\hat{\sigma}_M^2 = \sigma^2$), the bias corrected estimators almost perfectly match the underlying true values.

Next, we estimate the second moments of noise by our realized volatility estimators (RV) and, for comparison purposes, by the local averaging estimators (LA) proposed by Jacod et al. (2017b). We demonstrate the importance of the finite sample bias correction to obtain accurate estimates, and this applies to both estimators.¹¹ In Figure 3, we plot the means of the autocorrelations of noise estimated by RV and LA based on 1,000 simulations. In the top panel we plot the estimators without finite sample bias correction and we plot the estimators with finite sample bias correction in the bottom panel, in which we use the true σ^2 to make the bias correction. We will analyze the case in which σ^2 is estimated in the next subsection.

We observe that both estimators (RV and LA) perform poorly without finite sample bias correction. In particular, the noise autocorrelations estimated by the LA estimators decay slowly and hover above 0 up to 25 lags, from which we might conclude that the noise exhibits strong and long memory dependence, while the underlying noise is, in fact, only weakly dependent. However, both estimators perform well after the finite sample bias correction. In Figure 4, we also plot the 95% simulated confidence intervals of the two bias corrected estimators. In terms of mean squared errors, both estimators, after bias correction, yield accurate estimates. We note that the results for our RV estimator are robust to the choice of j_n .

Figures 2-4 reveal that the finite sample bias correction is crucial to obtain reliable estimates of noise moments. The key ingredient of this correction, however, is (an estimate of) the integrated volatility. Yet, to obtain an estimate of the integrated volatility, we need to estimate the second moments of noise first — whence the feedback loop of bias corrections. This is where our two-step estimators come into play.

6.3 Two-step estimators of integrated volatility and beyond

In this subsection, we examine the performance of our two-step estimators of integrated volatility. We will compare $\widehat{IV}_{\text{step1}}$ to $\widehat{IV}_{\text{step2}}$ (cf. (28) and (33)) to assess the gained accuracy by dropping the possibly misspecified assumption of independent noise, and compare \widehat{IV}_n to $\widehat{IV}_{\text{step2}}$ (cf. (24) and (33)) to assess the accuracy gains from the unified treatment of asymptotic and finite sample biases. We also illustrate the increased accuracy achieved by iterating one more step, yielding the estimator $\widehat{IV}_{\text{step3}}$.

In Table 1, we report the means of our estimators, with standard deviations between parentheses,

¹¹The finite sample bias corrected local averaging estimators of the noise covariances are given by

$$\widehat{R}(j)_n = \frac{1}{n} U((0, j))_n - \frac{K_n}{n} \left(\frac{4}{3} \hat{\sigma}^2 \right),$$

where $U((0, j))_n/n$ is the local averaging estimator of the j -th covariance without bias correction and $\hat{\sigma}^2$ is an estimator of the integrated volatility; see Jacod et al. (2017b) for more details. While Jacod et al. (2017b) provide a finite sample bias correction when developing their local averaging estimators of noise covariances, they don't consider the feedback between, and unified treatment of, asymptotic and finite sample biases, which is a key interest in this paper.

based on 1,000 simulations.¹² Throughout this subsection, j_n is fixed at 20. Upon comparing the first and the third rows, we observe the important advantage of our two-step estimators over the pre-averaging method that assumes independent noise, since our estimators yield strongly improved accuracy. Furthermore, a comparison between the results in the second and third rows leads to a striking conclusion: ignoring the finite sample bias yields even more inaccuracy than ignoring the dependence in noise! Thus one should be cautious in applying estimators without appropriate bias corrections even with data on a 1-sec time scale. The “cost” of applying our two-step estimators is the slightly larger standard deviations they induce. The increased uncertainty is introduced by correcting the “interlocked” bias. However, the reduction in bias strictly dominates the slight increase in standard deviations when noise is dependent. Therefore, the two-step estimator has smaller mean-squared errors than the other two estimators. The last row of Table 1 shows that another iteration of bias corrections yields even more accurate estimates, although the respective standard deviations increase slightly.

In Table 2, we replicate the results of Table 1 but now with higher data frequency (sampling at the 0.05-sec time scale). We clearly observe the inconsistency caused by the misspecification of the dependence structure in noise embedded in $\widehat{IV}_{\text{step1}}$ in the first row. The improved accuracy achieved by the estimator \widehat{IV}_n in the second row compared to the estimator $\widehat{IV}_{\text{step1}}$ in the first row confirms our asymptotic theory. However, interestingly we observe that, even with such ultra high-frequency data, the two-step estimator $\widehat{IV}_{\text{step2}}$ in the third row still performs better than the other two estimators — with smaller biases in most cases and only slightly larger standard deviations. In this scenario, one more iteration of bias corrections leads to little improvement.

Our results remain qualitatively the same when we increase the variance of noise. The relative improvement due to the 2-step estimator is even more pronounced in this case and a 3-step estimator may yield further improvements. As another robustness check, we also changed the exponentiated Ornstein-Uhlenbeck process for the efficient price process into a Geometric Brownian Motion. This only impacts the third digits of the estimates and the second digits of the standard deviations reported above.

To numerically “verify” the central limit theorem, we plot the quantiles of the normalized estimators $\frac{n^{1/4}(\widehat{IV}_n - \int_0^1 \sigma_s^2 ds)}{\tau_n}$, see (25), and the bias corrected version $\frac{n^{1/4}(\widehat{IV}_{\text{step2}} - \int_0^1 \sigma_s^2 ds)}{\tau_n}$ against standard normal quantiles in Figure 5. We observe that the limit distribution established in Theorem 4.2 is clearly verified.

In Appendix H, we provide additional Monte Carlo simulation evidence based on *stochastic volatility* models, using realistic parameters motivated by our empirical studies, and we find that our two-step estimator retains its advantage over the other two estimators, $\widehat{IV}_{\text{step1}}$ and \widehat{IV}_n .

¹²The numbers are multiplied by 10^5 .

7 Empirical Study

7.1 Data description

We analyze the NYSE TAQ transaction prices of Citigroup (trading symbol: C) over the month January 2011. We discard all transactions before 9:30 and after 16:00. We retain a total of 4,933,059 transactions over 20 trading days, thus on average 10.5 observations per second. The estimation is first performed on the full sample, and then on subsamples obtained by different sampling schemes. We demonstrate how the sampling methods affect the properties of the noise, and thus affect the estimation of the integrated volatility. Throughout this section, the tuning parameter of the RV estimator is fixed at $j_n = 30$ and $c = 0.2$.

7.2 Estimating the second moments of noise

We estimate the j -th autocovariance and autocorrelation of microstructure noise with $j = 0, 1, \dots, 30$ by three estimators: our realized volatility (RV) estimators in (8) and (9), the local averaging (LA) estimators proposed by [Jacod et al. \(2017b\)](#), and the bias corrected realized volatility (BCRV) estimators in (30) and (31). We perform the estimation over each trading day and end up with 20 estimates (of the 30 lags of autocovariances or autocorrelations) for each estimator. In [Figure 6](#) we plot the average of the 20 estimates (over the month) as well as the approximated confidence intervals that are two sample standard deviations away from the mean.

We observe that the three estimators yield quite close estimates by virtue of the high data frequency. Noise in this sample tends to be positively autocorrelated — with the BCRV estimators yielding the fastest decay. This is consistent with the finding that the arrivals of buy and sell orders are positively autocorrelated, see [Hasbrouck and Ho \(1987\)](#). This corresponds to the trading practice that informed traders split their orders over (a short period of) time and trade on one side of the market, rendering continuation in their orders.

We emphasize that the finite sample bias can be much more pronounced than what we observe in [Figure 6](#), even if we perform estimation on a full transaction data sample. In [Appendix I](#), we analyze the transaction prices of General Electric (GE) and show that, when the data frequency is very high, the finite sample bias correction is particularly important when the noise-to-signal ratio is very small (recall [Remark 3.3](#)).

7.3 Estimating the integrated volatility

Turning to the estimation of the integrated volatility, we mimic our simulation experiments and study three estimators: $\widehat{IV}_{\text{step1}}$, \widehat{IV}_n , and $\widehat{IV}_{\text{step2}}$. In the top panel of Figure 7, we plot the three estimators of the integrated volatility for each trading day. We note that the estimator \widehat{IV}_n and the two-step estimator $\widehat{IV}_{\text{step2}}$ yield quite close results. However, the estimator $\widehat{IV}_{\text{step1}}$, which ignores the dependence in noise, yields very different estimates, and the differences are one-sided — $\widehat{IV}_{\text{step1}}$ yields higher estimates over each trading day. Moreover, the differences are statistically significant by virtue of Theorem 4.2 — 19 out of the 20 estimates fall outside of the 95% confidence intervals, as the bottom panel of Figure 7 reveals.

7.4 Decaying rate of autocorrelation

Figure 6 shows that the positive autocorrelations of noise drop to zero rapidly. To assess the rate of decay, we perform a logarithmic transformation of the autocorrelations estimated by BCRV.¹³ In the top panel of Figure 8, we plot the logarithmic autocorrelations for each trading day, revealing clear support for a linear trend. To better visualize the linear relationship, we plot the means of the logarithmic autocorrelations over the 20 trading days and fit a regression line to it; see the bottom panel of Figure 8. The nearly perfect fit indicates that the logarithmic autocorrelation is approximately a linear function of the number of lags, i.e., the autocorrelation function is decaying at an exponential rate.¹⁴

7.5 Robustness check — estimation under other sampling schemes

It is interesting to analyze how our estimators perform when the data is sampled at different time scales. In this section, we consider two alternative (sub)sampling schemes: regular time sampling and tick time sampling (recall Remark 2.1 for details on the sampling schemes).

7.5.1 Regular time sampling

The prices in this sample are recorded on a 1-second time scale. If there were multiple prices in a second, we select the first one; and we do not record a price if there is no transaction in a second. We end up with 21,691 observations on average per trading day. Figure 9 is analogous to Figure 6. The three estimators, RV, LA, and BCRV, now produce very different patterns. Both the RV and LA estimators indicate that noise is strongly autocorrelated in this subsample, even stronger than in the original full sample. This would be counterintuitive since we eliminate more than 90% of the full sample in a fairly random way —

¹³We restrict attention to the lags up to $j = 15$. The logarithmic autocorrelations at higher lags are very volatile since the autocorrelations are close to zero.

¹⁴The autocorrelation decay rate would be slower without unified treatment of the bias corrections, which may explain the polynomial dependence in noise found in Jacod et al. (2017b) and questioned by these authors themselves.

the elimination should if anything have weakened the serial dependence of noise in the remaining sample. However, the estimates by BCRV reveal that in fact the noise is approximately uncorrelated — it is the finite sample bias that makes the autocorrelations of noise seem strong and persistent if not taken into account.

If the noise is close to being independent, $\widehat{IV}_{\text{step1}}$, which assumes i.i.d. noise, would be a valid estimator of the integrated volatility. An alternative estimator, e.g., $\widehat{IV}_{\text{step2}}$ or \widehat{IV}_n , would be robust if it delivered similar estimates. In the top panel of Figure 10, we observe that $\widehat{IV}_{\text{step1}}$ and $\widehat{IV}_{\text{step2}}$ yield virtually identical estimates. The estimator \widehat{IV}_n , however, yields lower estimates on each trading day. If we rely on the asymptotic theory only, we would conclude that the estimates by $\widehat{IV}_{\text{step1}}$ (or $\widehat{IV}_{\text{step2}}$) are significantly higher than those by \widehat{IV}_n in the statistical sense — all the 20 estimates by $\widehat{IV}_{\text{step1}}$ (or $\widehat{IV}_{\text{step2}}$) are outside the 95% asymptotic confidence intervals of \widehat{IV}_n , as we observe from the bottom panel of Figure 10. We conclude that Figures 7 and 10 jointly reveal the importance of our multi-step approach. Indeed, $\widehat{IV}_{\text{step1}}$ shows unreliable behaviour in Figure 7, while \widehat{IV}_n shows unreliable behaviour in Figure 10.

7.5.2 Tick time sampling

In a tick time sample, prices are collected with each price change, i.e., all zero returns are suppressed, see, e.g., Da and Xiu (2017), Aït-Sahalia et al. (2011), Griffin and Oomen (2008), Kalnina (2011) and Zhou (1996). For the Citigroup transaction data, 70% of the returns are zero. The corresponding average number of prices per second in our tick time sample is 3.2. Figure 11 shows that the microstructure noise has a different dependence pattern in the tick time sample — its autocorrelation function is alternating. Masked by alternating noise, the observed returns at tick time have a similar pattern; see Aït-Sahalia et al. (2011) and Griffin and Oomen (2008). This dependence structure of noise is perceived to be due to the discreteness of price changes, irrespective of the distributional features of noise in the original transactions or quotes data.

Interestingly, Figure 12 shows that the three estimators of the integrated volatility, $\widehat{IV}_{\text{step1}}$, $\widehat{IV}_{\text{step2}}$, and \widehat{IV}_n , remain close. It is not surprising to see a close fit of $\widehat{IV}_{\text{step2}}$ and \widehat{IV}_n since the data frequency is still quite high. By contrast, it is not directly obvious why $\widehat{IV}_{\text{step1}}$ and $\widehat{IV}_{\text{step2}}$ deliver almost identical estimates, given the fact that the dependence of noise in this tick time sample is drastically different from i.i.d. noise. However, a clue is provided by the observation that negatively autocorrelated noise has less impact on the estimation of the integrated volatility, as the high-order alternating autocovariances partially cancel out, thus contributing less to the asymptotic bias σ_U^2 .¹⁵

¹⁵For a tractable analysis, one may consider AR(1) noise processes. Let $\rho \in (0, 1)$ be the absolute value of the AR(1) coefficient. When the noise is positively autocorrelated, the asymptotic bias σ_U^2 corrected by $\widehat{IV}_{\text{step1}}$ and $\widehat{IV}_{\text{step2}}$ is $(1 -$

7.6 Economic interpretation and empirical implication

The dependence structure of microstructure noise is complex, and depends on the sampling scheme. In an original transaction data sample, noise is likely to be positively autocorrelated as a result of various trading practices that entail continuation in order flows. The dependence of noise can be reduced by sampling sparsely, say, every few (or more) seconds as we show in Section 7.5.1; noise is close to independent in such sparse subsamples. If, however, we remove all zero returns, thus sample in tick time, noise typically exhibits an alternating autocorrelogram.

Microstructure theories can provide some intuitive economic interpretations of the dynamic properties of microstructure noise recovered in this paper. The positive autocorrelation function displayed in Figure 6 is consistent with the findings in Hasbrouck and Ho (1987), Choi et al. (1988) and Huang and Stoll (1997) that explicitly model the probability of order reversal π (or order continuation by $1 - \pi$),¹⁶ so that the deviation of transaction prices from fundamentals becomes an AR(1) process. Fitting the autocorrelation function recovered by BCRV in Figure 6 to that of an AR(1) model, we obtain an estimate of the AR(1) coefficient equal to $\hat{\rho} = 0.75$ and the probability of order continuation is $1 - \hat{\pi} = (1 + \hat{\rho})/2 = 0.87$. That is, the estimated probability that a buy (or sell) order follows another buy (or sell) order is 0.87. In view of the extensive empirical results in Huang and Stoll (1997) (see Table 5 therein), this is a reasonable estimate.

One possible interpretation of the positively autocorrelated order flows is that a large *order* is often executed as a series of smaller *trades* to reduce the price impact, or conducted against multiple *trades* from stale limit orders. However, such positive autocorrelation contradicts the prediction of inventory models, in which market makers induce negatively autocorrelated order flows to stabilize inventories; see Ho and Stoll (1981). Consequently, according to inventory models the probability of order reversal would be $\pi > 0.5$. One remedy, suggested by Huang and Stoll (1997), is to collapse multiple *trades* at the same price into one *order*, which is exactly the tick time sampling scheme considered in Section 7.5.2. Exploiting the estimates by BCRV presented in Figure 11, we obtain an estimate of the probability of order reversal equal to $\hat{\pi} = 0.84$, which is very close to the average probability 0.87 in Huang and Stoll (1997). We emphasize that we recover these probabilities without any prior knowledge or estimates of the order flows.

The dependence structure of microstructure noise, and hence the choice of sampling scheme, affect the $\rho \mathbf{Var}(U)$ and $\frac{1+\rho}{1-\rho} \mathbf{Var}(U)$, respectively; when the noise is negatively autocorrelated, it is $(1 + \rho) \mathbf{Var}(U)$ and $\frac{1-\rho}{1+\rho} \mathbf{Var}(U)$. Consider $\rho = 0.8$. Then, $(1 - \rho) \mathbf{Var}(U) = 0.2 \mathbf{Var}(U)$ and $\frac{1+\rho}{1-\rho} \mathbf{Var}(U) = 9 \mathbf{Var}(U)$ while $(1 + \rho) \mathbf{Var}(U) = 1.8 \mathbf{Var}(U)$ and $\frac{1-\rho}{1+\rho} \mathbf{Var}(U) = \frac{1}{9} \mathbf{Var}(U)$. Therefore, the difference in the asymptotic bias is smaller when the noise is negatively autocorrelated; consequently, the integrated volatility estimates by $\widehat{IV}_{\text{step1}}$ and $\widehat{IV}_{\text{step2}}$ are close. See also Tables 1 and 2 in our simulation study.

¹⁶It is the probability that a buy (sell) order follows another sell (buy) order.

estimation of integrated volatility. Popular de-noise methods that assume i.i.d. noise work reasonably well with relatively sparse regular time samples or tick time samples. However, this discards a substantial amount of the original transaction data.¹⁷ Instead, we can directly estimate the integrated volatility from the original transaction data using our estimators that explicitly take the potential dependence in noise into account.

In our empirical study, we have also illustrated that bias corrections play an essential role in recovering the statistical properties of noise and in estimating the integrated volatility. Our two-step estimators are specifically designed to conduct such bias corrections, and have the advantage of being robust to different sampling schemes and frequencies.

8 Conclusion

In high-frequency financial data the efficient price is contaminated by microstructure noise, which is usually assumed to be independently and identically distributed. This simple distributional assumption is challenged by both microeconomic financial models and various empirical facts. In this paper, we deviate from the i.i.d. assumption by allowing noise to be dependent in a general setting. We then develop econometric tools to recover the dynamic properties of microstructure noise and design improved approaches for the estimation of the integrated volatility.

This paper makes four contributions. First, it develops nonparametric estimators of the second moments of microstructure noise in a general setting. Second, it provides a robust estimator of the integrated volatility, without assuming serially independent noise. Third, it reveals the importance of both asymptotic and finite sample bias analysis and develops simple and readily implementable two-step estimators that are robust to the sampling frequency. Empirically, it characterizes the dependence structures of noise in several popular sampling schemes and provides intuitive economic interpretations; it also investigates the impact of the dynamic properties of microstructure noise on integrated volatility estimation.

This paper thus introduces a robust and accurate method to effectively separate the two components of high-frequency financial data — the efficient price and microstructure noise. The robustness lies in its flexibility to accommodate rich dependence structures of microstructure noise motivated by various economic models and trading practices, whereas the accuracy is achieved by the finite sample refinement. As a result, we discover dynamic properties of microstructure noise consistent with microstructure theory and obtain accurate volatility estimators that are robust to sampling schemes.

¹⁷To obtain the Citigroup tick time sample and the 1-second regular time sample, we delete roughly 70% and 90% of the original transaction data, respectively.

Acknowledgements

We are very grateful to Yacine Aït-Sahalia, Federico Bandi, Peter Boswijk, Peter Reinhard Hansen, Siem Jan Koopman, Oliver Linton, and Xiye Yang for their comments and discussions on earlier versions of this paper. This research was funded in part by the Netherlands Organization for Scientific Research under grant NWO VIDI 2009 (Laeven).

References

- AÏT-SAHALIA, Y. AND J. JACOD (2014): *High-frequency Financial Econometrics*, Princeton University Press.
- AÏT-SAHALIA, Y., P. A. MYKLAND, AND L. ZHANG (2005): “How often to sample a continuous-time process in the presence of market microstructure noise,” *Review of Financial Studies*, 18, 351–416.
- (2011): “Ultra high frequency volatility estimation with dependent microstructure noise,” *Journal of Econometrics*, 160, 160–175.
- BANDI, F. M. AND J. R. RUSSELL (2006): “Separating microstructure noise from volatility,” *Journal of Financial Economics*, 79, 655–692.
- (2008): “Microstructure noise, realized variance, and optimal sampling,” *Review of Economic Studies*, 75, 339–369.
- BARNDORFF-NIELSEN, O. E., S. E. GRAVERSEN, J. JACOD, M. PODOLSKIJ, AND N. SHEPHARD (2006): “A central limit theorem for realised power and bipower variations of continuous semimartingales,” in *From Stochastic Calculus to Mathematical Finance*, ed. by Y. Kabanov, R. Lipster, and J. Stoyanov, Springer.
- BARNDORFF-NIELSEN, O. E., P. R. HANSEN, A. LUNDE, AND N. SHEPHARD (2008): “Designing realized kernels to measure the ex post variation of equity prices in the presence of noise,” *Econometrica*, 76, 1481–1536.
- BLACK, F. (1986): “Noise,” *Journal of Finance*, 41, 529–543.
- BRADLEY, R. C. (2005): “Basic properties of strong mixing conditions. A survey and some open questions,” *Probability Surveys*, 2, 107–144.
- (2007): *Introduction to Strong Mixing Conditions*, Kendrick Press.

- CHOI, J. Y., D. SALANDRO, AND K. SHASTRI (1988): “On the estimation of bid-ask spreads: Theory and evidence,” *Journal of Financial and Quantitative Analysis*, 23, 219–230.
- CHRISTENSEN, K., R. C. OOMEN, AND M. PODOLSKIJ (2014): “Fact or friction: Jumps at ultra high frequency,” *Journal of Financial Economics*, 114, 576–599.
- CHUNG, K. L. (2001): *A Course in Probability Theory*, Academic Press.
- DA, R. AND D. XIU (2017): “When Moving-Average Models Meet High-Frequency Data: Uniform Inference on Volatility,” Tech. rep.
- DUFFIE, D. (2010): *Dynamic Asset Pricing Theory*, Princeton University Press.
- GARMAN, M. B. (1976): “Market microstructure,” *Journal of Financial Economics*, 3, 257–275.
- GLOSTEN, L. R. AND P. R. MILGROM (1985): “Bid, ask and transaction prices in a specialist market with heterogeneously informed traders,” *Journal of Financial Economics*, 14, 71–100.
- GRIFFIN, J. E. AND R. C. OOMEN (2008): “Sampling returns for realized variance calculations: tick time or transaction time?” *Econometric Reviews*, 27, 230–253.
- GROSS-KLUSSMANN, A. AND N. HAUTSCH (2013): “Predicting bid–ask spreads using long-memory autoregressive conditional Poisson models,” *Journal of Forecasting*, 32, 724–742.
- HANSEN, P. R., J. LARGE, AND A. LUNDE (2008): “Moving average-based estimators of integrated variance,” *Econometric Reviews*, 27, 79–111.
- HANSEN, P. R. AND A. LUNDE (2006): “Realized variance and market microstructure noise,” *Journal of Business & Economic Statistics*, 24, 127–161.
- HARRIS, L. (1990): “Estimation of stock price variances and serial covariances from discrete observations,” *Journal of Financial and Quantitative Analysis*, 25, 291–306.
- HASBROUCK, J. (2007): *Empirical Market Microstructure: The Institutions, Economics, and Econometrics of Securities Trading*, Oxford University Press.
- HASBROUCK, J. AND T. S. HO (1987): “Order arrival, quote behavior, and the return-generating process,” *Journal of Finance*, 42, 1035–1048.
- HAUTSCH, N. AND M. PODOLSKIJ (2013): “Preaveraging-based estimation of quadratic variation in the presence of noise and jumps: Theory, implementation, and empirical evidence,” *Journal of Business & Economic Statistics*, 31, 165–183.

- HENDERSHOTT, T., C. JONES, AND A. J. MENKVELD (2013): “Implementation shortfall with transitory price effects,” *High Frequency Trading: New Realities for Trades, Markets and Regulators*, Easley, D., M. Lopez de Prado, and M. O’Hara (editors), Risk Books (London: 2013).
- HO, T. AND H. R. STOLL (1981): “Optimal dealer pricing under transactions and return uncertainty,” *Journal of Financial Economics*, 9, 47–73.
- HUANG, R. D. AND H. R. STOLL (1997): “The components of the bid-ask spread: A general approach,” *Review of Financial Studies*, 10, 995–1034.
- JACOD, J., Y. LI, P. A. MYKLAND, M. PODOLSKIJ, AND M. VETTER (2009): “Microstructure noise in the continuous case: The pre-averaging approach,” *Stochastic Processes and Their Applications*, 119, 2249–2276.
- JACOD, J., Y. LI, AND X. ZHENG (2017a): “Estimating the integrated volatility with tick observations,” Tech. rep.
- (2017b): “Statistical properties of microstructure noise,” *Econometrica*, 85, 1133–1174.
- JACOD, J., M. PODOLSKIJ, AND M. VETTER (2010): “Limit theorems for moving averages of discretized processes plus noise,” *Annals of Statistics*, 38, 1478–1545.
- JACOD, J. AND P. E. PROTTER (2011): *Discretization of Processes*, vol. 67, Springer Science & Business Media.
- JACOD, J. AND A. N. SHIRYAEV (2003): *Limit Theorems for Stochastic Processes*, vol. 288, Springer-Verlag Berlin.
- KALNINA, I. (2011): “Subsampling high frequency data,” *Journal of Econometrics*, 161, 262–283.
- LEE, S. S. AND P. A. MYKLAND (2012): “Jumps in equilibrium prices and market microstructure noise,” *Journal of Econometrics*, 168, 396–406.
- LI, Z. M., R. J. A. LAEVEN, AND M. H. VELLEKOOP (2018): “Supplementary material to “Dependent microstructure noise and integrated volatility estimation from high-frequency data,” Tech. rep.
- MOKKADEM, A. (1988): “Mixing properties of ARMA processes,” *Stochastic Processes and Their Applications*, 29, 309–315.
- PODOLSKIJ, M. AND M. VETTER (2009a): “Bipower-type estimation in a noisy diffusion setting,” *Stochastic Processes and Their Applications*, 119, 2803–2831.

- (2009b): “Estimation of volatility functionals in the simultaneous presence of microstructure noise and jumps,” *Bernoulli*, 15, 634–658.
- ROLL, R. (1984): “A simple implicit measure of the effective bid-ask spread in an efficient market,” *Journal of Finance*, 39, 1127–1139.
- STOLL, H. R. (1989): “Inferring the components of the bid-ask spread: theory and empirical tests,” *the Journal of Finance*, 44, 115–134.
- TSAY, R. S. (2005): *Analysis of Financial Time Series*, vol. 543, John Wiley & Sons.
- WHITE, H. (2000): *Asymptotic Theory for Econometricians*, Academic Press.
- XIU, D. (2010): “Quasi-maximum likelihood estimation of volatility with high frequency data,” *Journal of Econometrics*, 159, 235–250.
- ZHANG, L. (2006): “Efficient estimation of stochastic volatility using noisy observations: A multi-scale approach,” *Bernoulli*, 12, 1019–1043.
- ZHANG, L., P. A. MYKLAND, AND Y. AÏT-SAHALIA (2005): “A tale of two time scales: Determining integrated volatility with noisy high-frequency data,” *Journal of the American Statistical Association*, 100, 1394–1411.
- ZHOU, B. (1996): “High-frequency data and volatility in foreign-exchange rates,” *Journal of Business & Economic Statistics*, 14, 45–52.

Tables and Figures

ρ	-0.7	-0.3	0	0.3	0.7
$\widehat{IV}_{\text{step1}}$	5.53 (0.46)	5.74 (0.46)	5.98 (0.47)	6.39 (0.49)	7.57 (0.56)
\widehat{IV}_n	3.04 (0.40)	3.02 (0.40)	3.02 (0.41)	3.04 (0.43)	2.91 (0.50)
$\widehat{IV}_{\text{step2}}$	5.79 (0.61)	5.87 (0.63)	5.99 (0.63)	6.23 (0.67)	6.67 (0.76)
$\widehat{IV}_{\text{step3}}$	5.92 (0.70)	5.93 (0.72)	6.00 (0.72)	6.13 (0.76)	6.22 (0.87)

Table 1: Estimation of the integrated volatility. The numbers represent the means of the four estimators of integrated volatility, $\widehat{IV}_{\text{step1}}$, \widehat{IV}_n , $\widehat{IV}_{\text{step2}}$ and $\widehat{IV}_{\text{step3}}$, based on 1,000 simulations with standard deviations between parentheses. The true value of the integrated volatility is given by $\sigma^2 = 6 \times 10^{-5}$. All numbers in the table are multiplied by 10^5 . We take $\Delta = 1$ sec and the number of observations is 23,400. The tuning parameter of the RV estimator is $j_n = 20$ and $i_n = 10$.

ρ	-0.7	-0.3	0	0.3	0.7
$\widehat{IV}_{\text{step1}}$	5.52 (0.22)	5.76 (0.21)	6.00 (0.22)	6.37 (0.23)	7.71 (0.27)
\widehat{IV}_n	5.86 (0.22)	5.85 (0.21)	5.85 (0.22)	5.84 (0.23)	5.88(0.27)
$\widehat{IV}_{\text{step2}}$	5.99 (0.23)	6.00 (0.22)	6.00 (0.23)	6.00 (0.24)	6.07 (0.27)
$\widehat{IV}_{\text{step3}}$	6.00 (0.23)	6.00 (0.22)	6.00 (0.23)	5.99 (0.24)	6.03 (0.27)

Table 2: Estimation of the integrated volatility with ultra high-frequency data. The numbers represent the means of the four estimators of integrated volatility, $\widehat{IV}_{\text{step1}}$, \widehat{IV}_n , $\widehat{IV}_{\text{step2}}$ and $\widehat{IV}_{\text{step3}}$, based on 1,000 simulations with standard deviations between parentheses. The true value of the integrated volatility is given by $\sigma^2 = 6 \times 10^{-5}$. All numbers in the table are multiplied by 10^5 . Different from Table 1, we now take $\Delta = 0.05$ sec and the number of observations is 468,000. The tuning parameter of the RV estimator is $j_n = 20$ and $i_n = 10$.

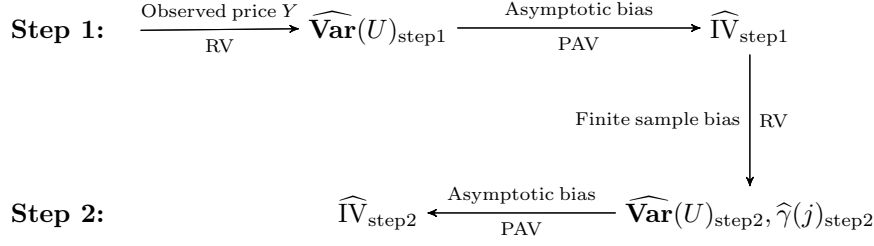


Figure 1: Illustration of the two-step estimators. In the first step, we use realized volatility (RV) to obtain an estimator of the variance of (possibly misspecified) i.i.d. noise, $\widehat{\mathbf{Var}}(U)_{\text{step1}}$. Next, this estimator is used to correct the asymptotic bias in the probability limit of the pre-averaging estimator (PAV) to derive the first-step estimator of the integrated volatility, $\widehat{\mathbf{IV}}_{\text{step1}}$. In the second step, we use $\widehat{\mathbf{IV}}_{\text{step1}}$ to obtain finite sample bias corrected estimators of the variance and covariances of noise, $\widehat{\mathbf{Var}}(U)_{\text{step2}}$ and $\widehat{\gamma}(j)_{\text{step2}}$, which are finally used to remove the asymptotic bias in PAV, leading to the second-step integrated volatility estimator, $\widehat{\mathbf{IV}}_{\text{step2}}$.

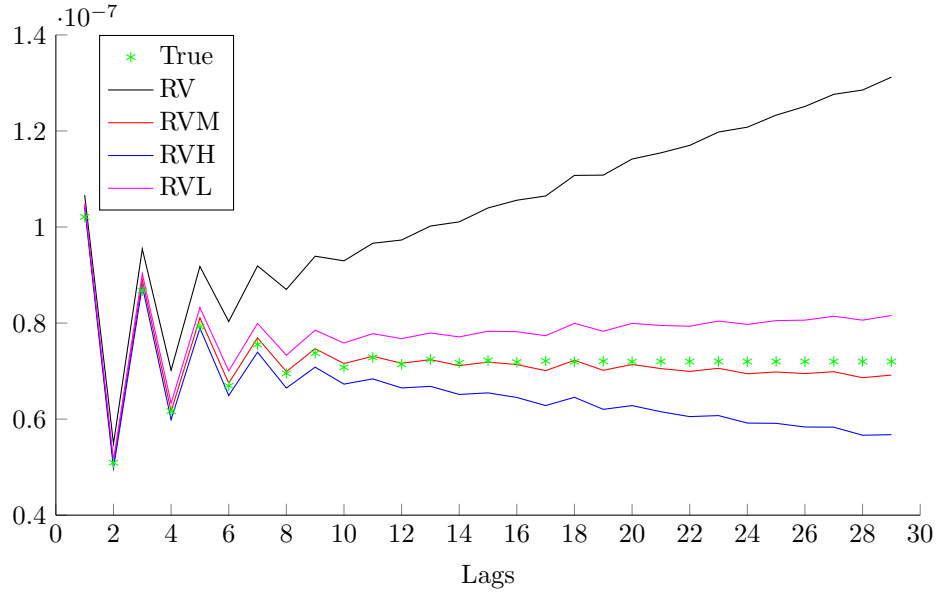


Figure 2: Realized volatility estimators against the number of lags j , based on a single simulated sample, without and with finite sample bias correction, cf. (7) and (11). Here, RV: $\widehat{\langle Y, Y \rangle}_n(j)$; RVL: $\widehat{\langle Y, Y \rangle}_n(j) - \frac{0.8\sigma^2 j}{2(n-j+1)}$; RVM: $\widehat{\langle Y, Y \rangle}_n(j) - \frac{\sigma^2 j}{2(n-j+1)}$; and RVH: $\widehat{\langle Y, Y \rangle}_n(j) - \frac{1.2\sigma^2 j}{2(n-j+1)}$. We take $\Delta = 1$ sec, the number of observations is 23,400, and $\rho = -0.7$. The designation “True” corresponds to the stochastic limit $\mathbf{Var}(U) - \gamma(j)$.

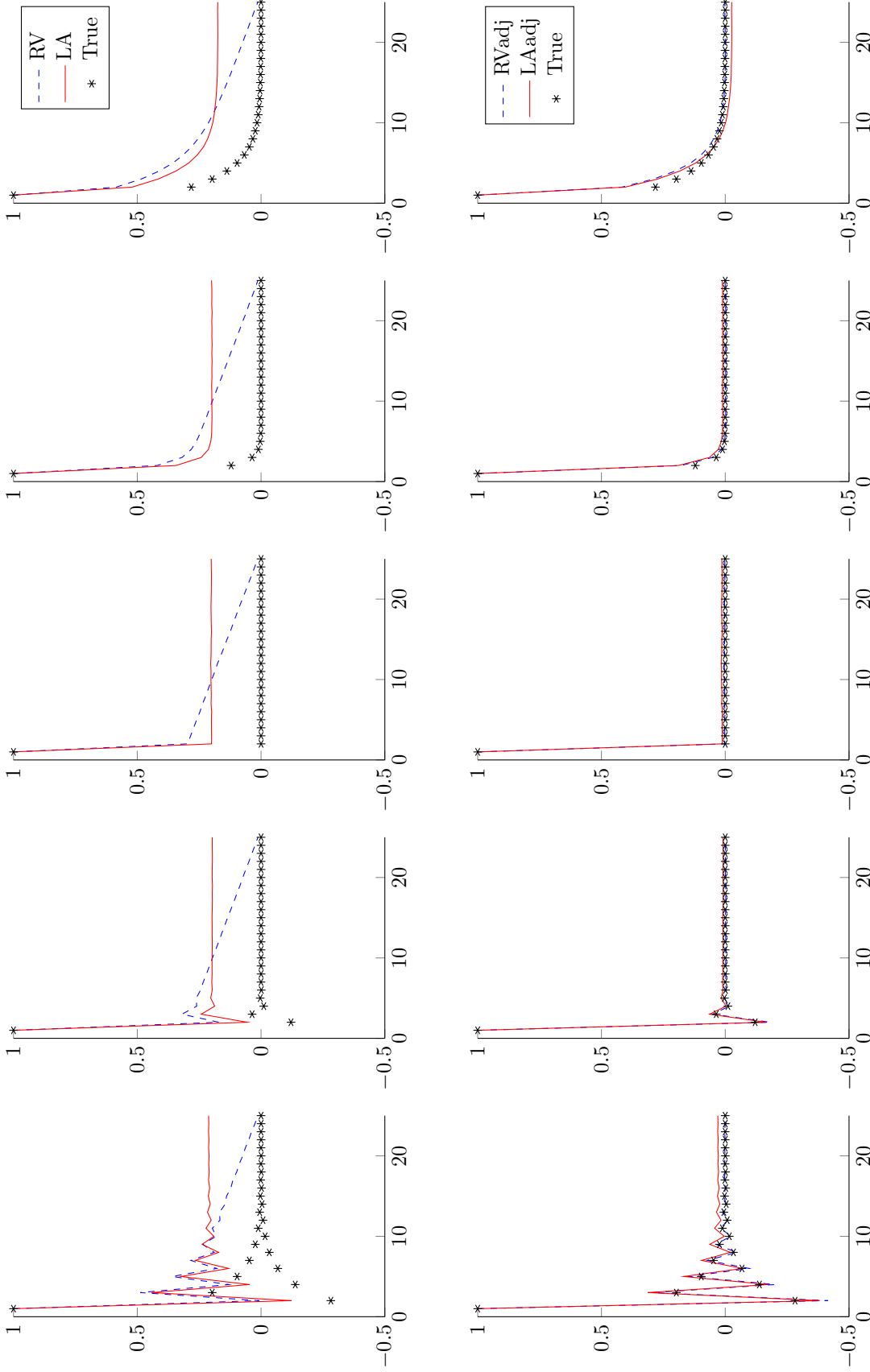


Figure 3: Realized volatility (RV) and local averaging (LA) estimators of the autocorrelations of noise against the number of lags j , averaged over 1,000 simulated samples. Top panel: RV and LA estimators without finite sample bias corrections. Bottom panel: RV and LA estimators with finite sample bias corrections. We take $\Delta = 1$ sec and the number of observations is 23,400. The tuning parameters of the RV and LA estimators are $j_n = 25$ and $K_n = 6$, respectively. The AR(1) coefficient ρ of the noise process is fixed in each column. From left to right, the values of ρ for each column are given by -0.7 , -0.3 , 0 , 0.3 , and 0.7 .

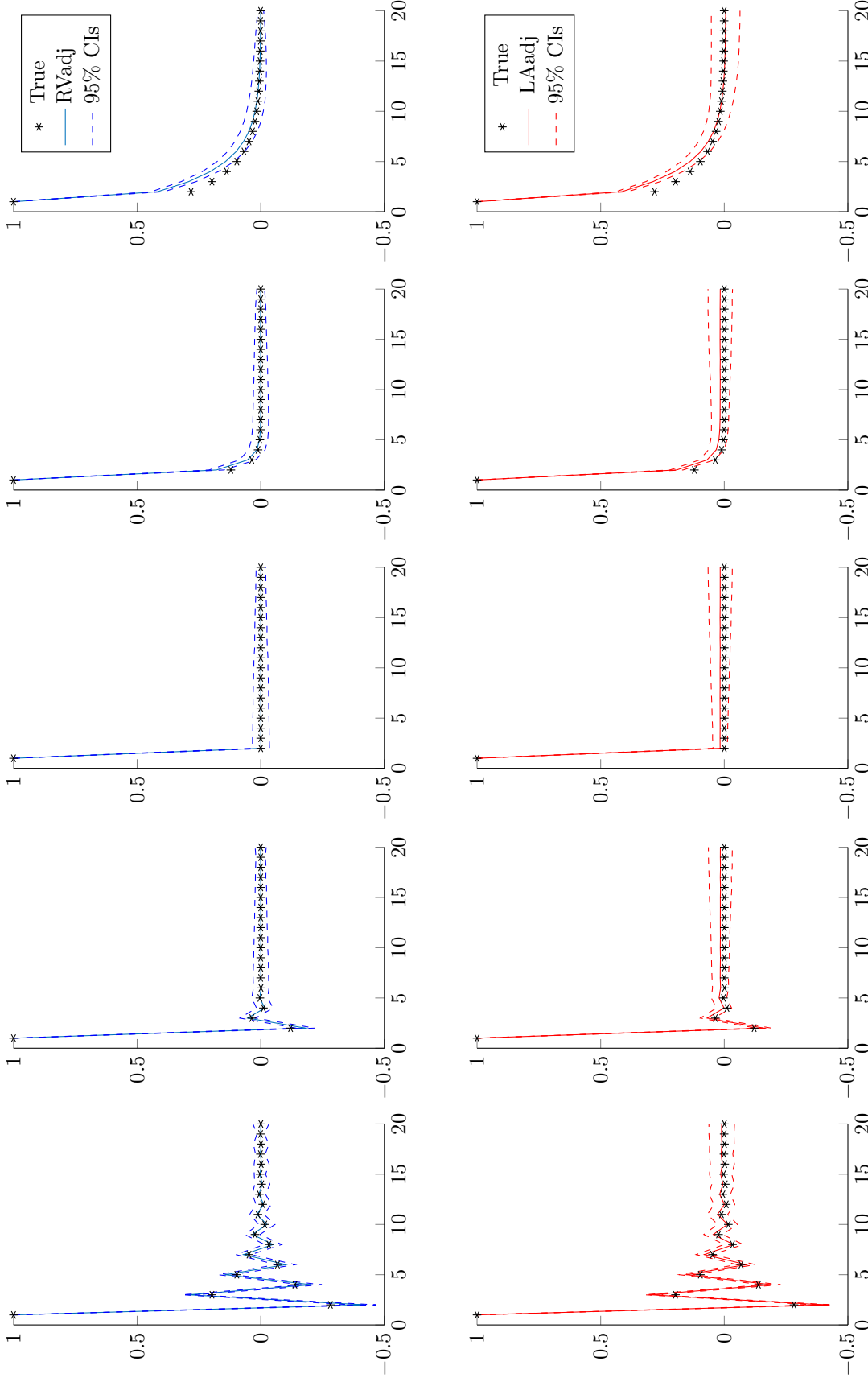


Figure 4: Realized volatility (RV) and local averaging (LA) estimators of the autocorrelations of noise against the number of lags j , averaged over 1,000 simulated samples. Top panel: RV estimators of the autocorrelations of noise (solid) with 95% simulated confidence intervals (dashed). Bottom panel: LA estimators of the autocorrelations of noise (solid) with 95% simulated confidence intervals (dashed). The true autocorrelations are displayed in stars. Both estimators include the finite sample bias correction. We take $\Delta = 1$ sec and the number of observations is 23,400. The tuning parameters of the RV and LA estimators are $j_n = 20$ and $K_n = 6$, respectively. The AR(1) coefficient ρ of the noise process is fixed in each column. From left to right, the values of ρ for each column are given by $-0.7, -0.3, 0, 0.3$, and 0.7 .

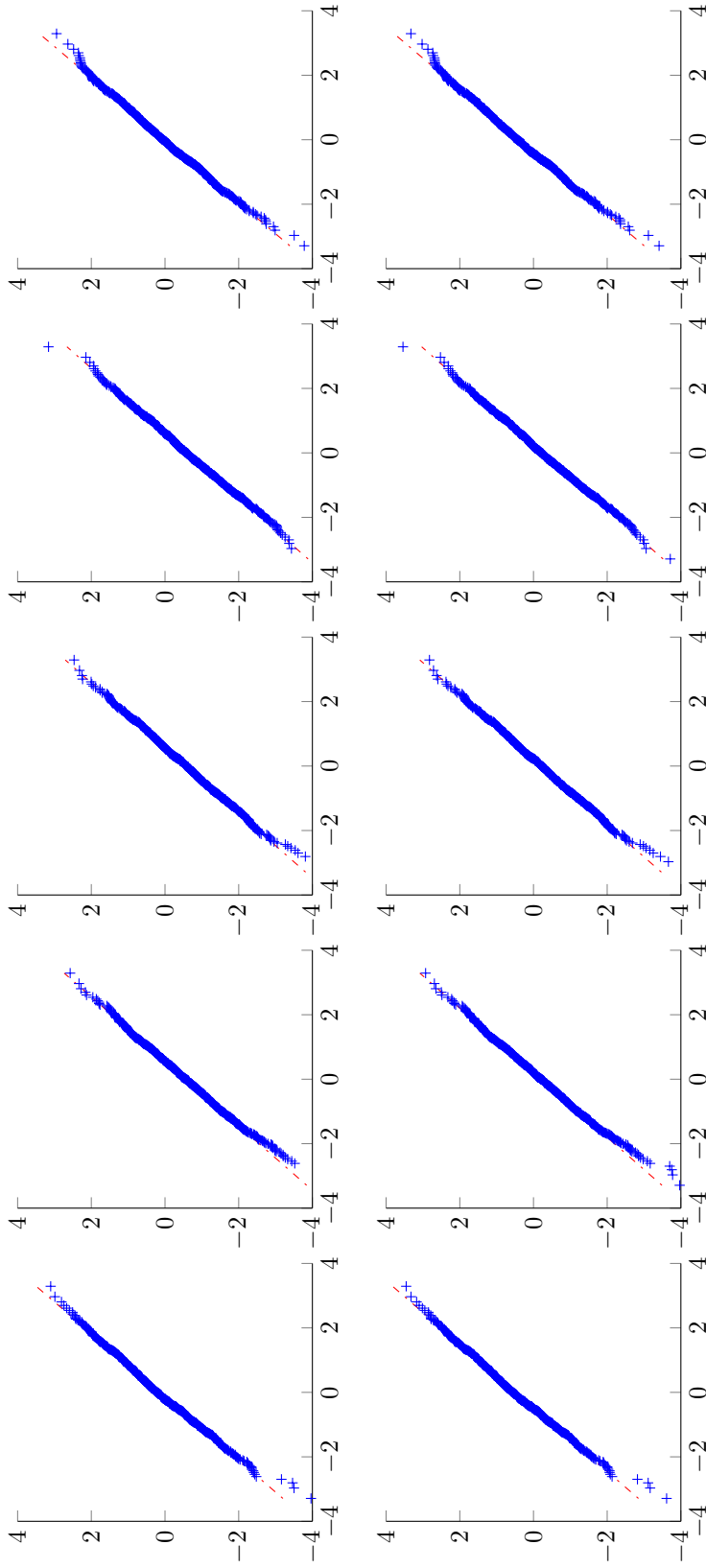


Figure 5: Top panel: Standard normal QQ-plots of $n^{1/4} \left(\widehat{IV}_n - \int_0^1 \sigma_s^2 ds \right) / \tau_n$. Bottom panel: Standard normal QQ-plots of $n^{1/4} \left(\widehat{IV}_{step2} - \int_0^1 \sigma_s^2 ds \right) / \tau_n$. The AR(1) coefficient ρ of the noise process is fixed in each column. From left to right, the values of ρ for each column are given by $-0.7, -0.3, 0, 0.3$, and 0.7 . The number of simulations is 1,000, the data frequency is $\Delta = 0.05$ sec, and the number of observations is 468,000. The tuning parameter of the RV estimator is $j_n = 20$ and $i_n = 10$.

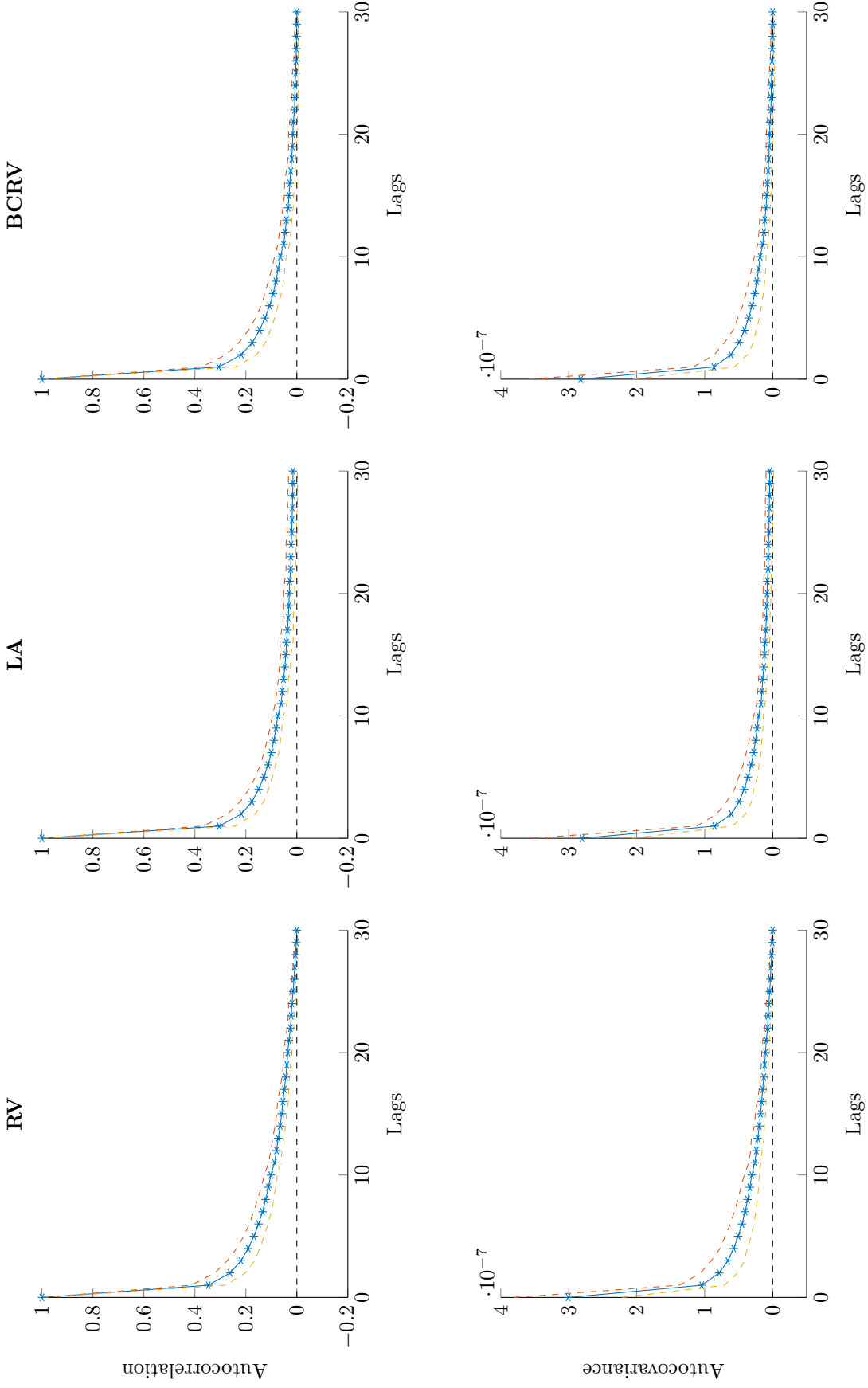


Figure 6: From the left to the right, we display the realized volatility (RV), local averaging (LA), and the bias corrected realized volatility (BCRV) estimators of the autocorrelations (top panel) and autocovariances (bottom panel) of noise against the number of lags j based on transaction data for Citigroup. Sample period: January, 2011. On average there are 10.5 observations per second in the sample. The three estimators are applied to and next averaged over each of the 20 trading days. The stars indicate the means of the 20 estimates. The dashed lines are 2 standard deviations away from the mean. The tuning parameter of the RV estimator is $j_n = 30$.

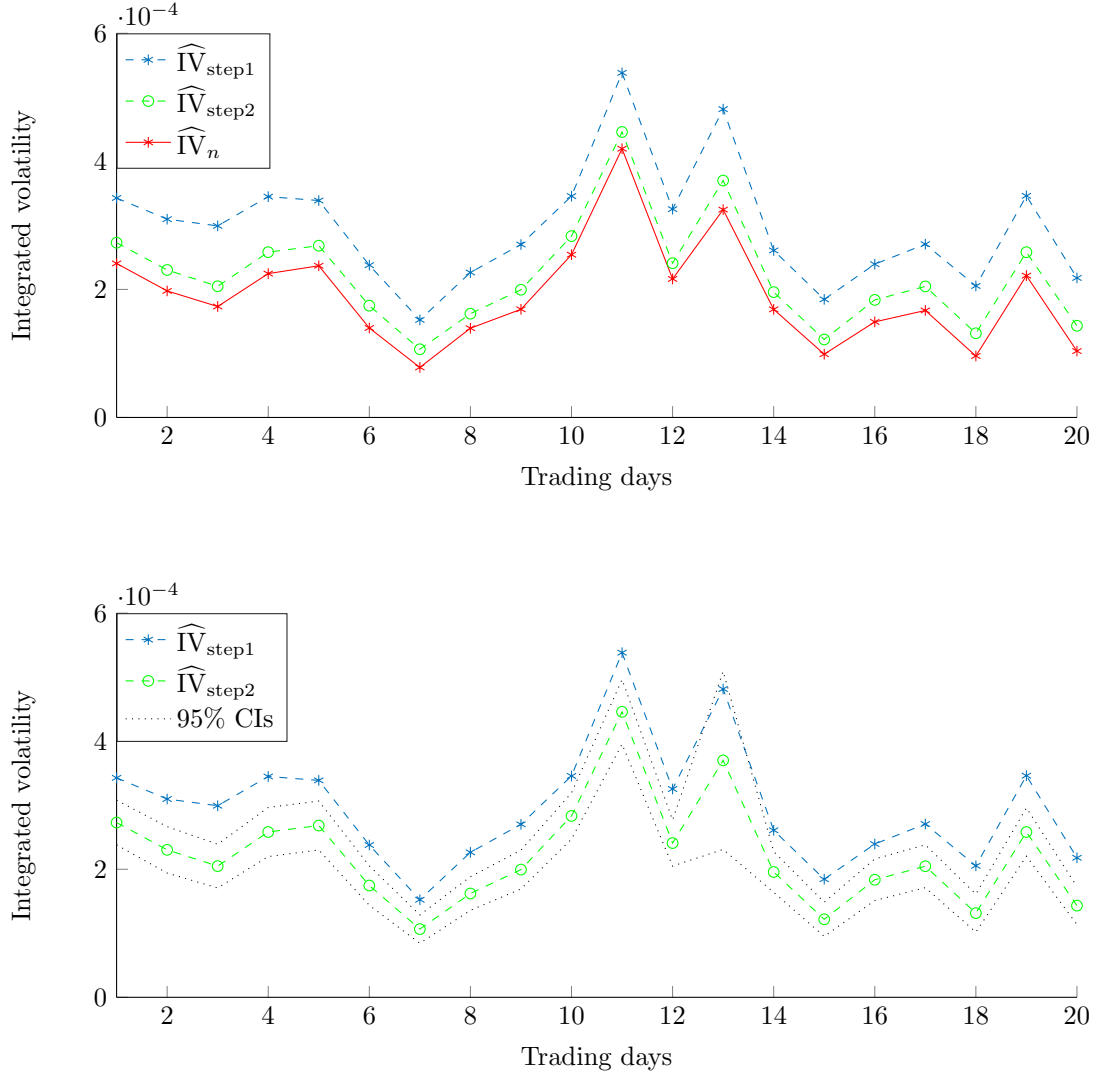


Figure 7: Estimation of the integrated volatility based on transaction data for Citigroup. Sample period: January, 2011, consisting of 20 trading days. On average there are 10.5 observations per second in the sample. The estimators $\widehat{IV}_{\text{step1}}$, $\widehat{IV}_{\text{step2}}$, and \widehat{IV}_n are given by (28), (33), and (23). In the bottom panel, the asymptotic confidence intervals (CIs) are based on the limit distribution in Theorem 4.2. The tuning parameter of the RV estimator is $j_n = 30$ and $i_n = 15$.

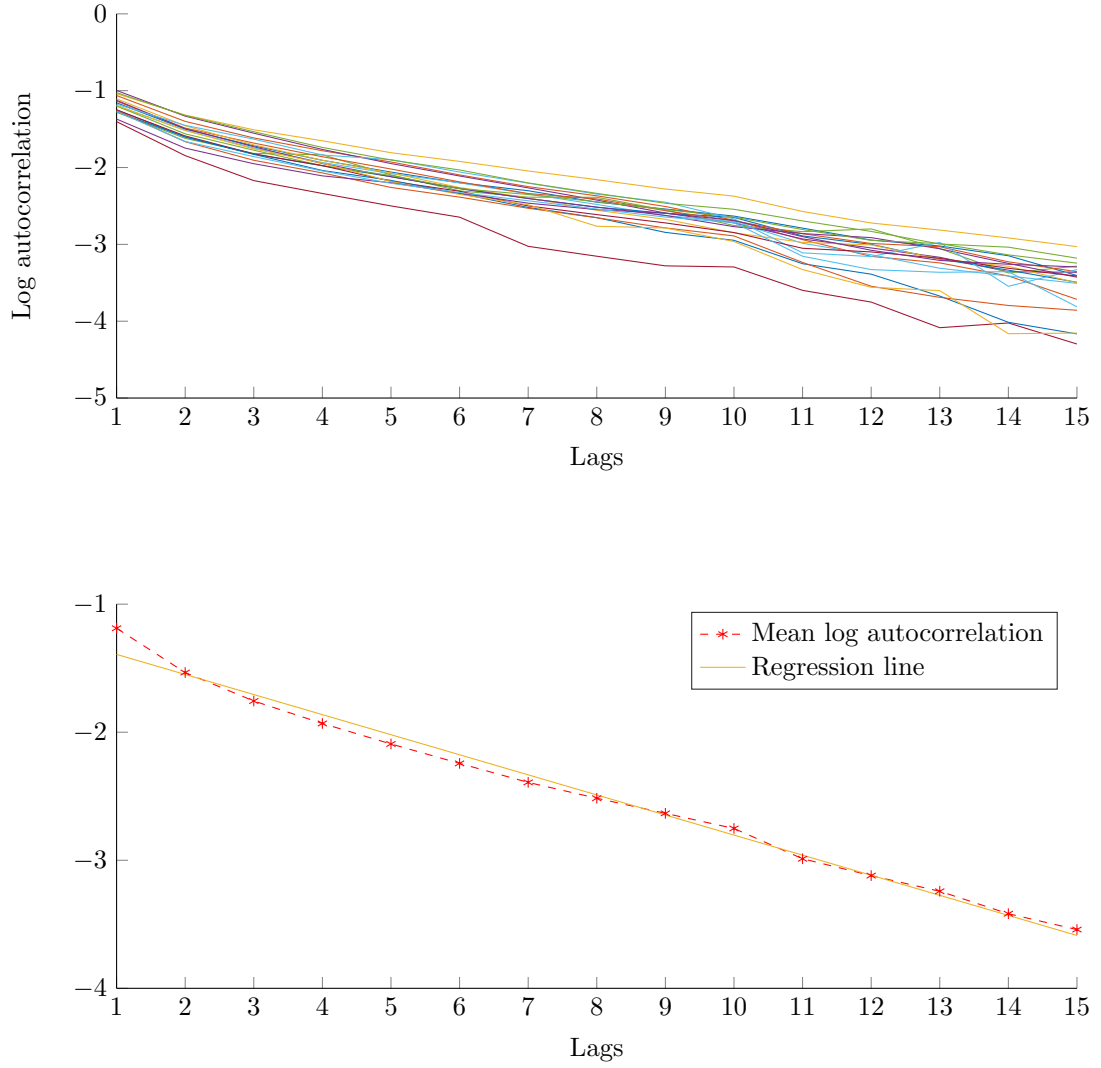


Figure 8: Top panel: Logarithmic autocorrelations of noise against the number of lags j estimated by BCRV for each trading day based on transaction data for Citigroup. Bottom panel: Means of the logarithmic autocorrelations of noise and a linear regression line. Sample period: January, 2011, consisting of 20 trading days. On average there are 10.5 observations per second in the sample. The tuning parameter of the RV estimator is $j_n = 30$.

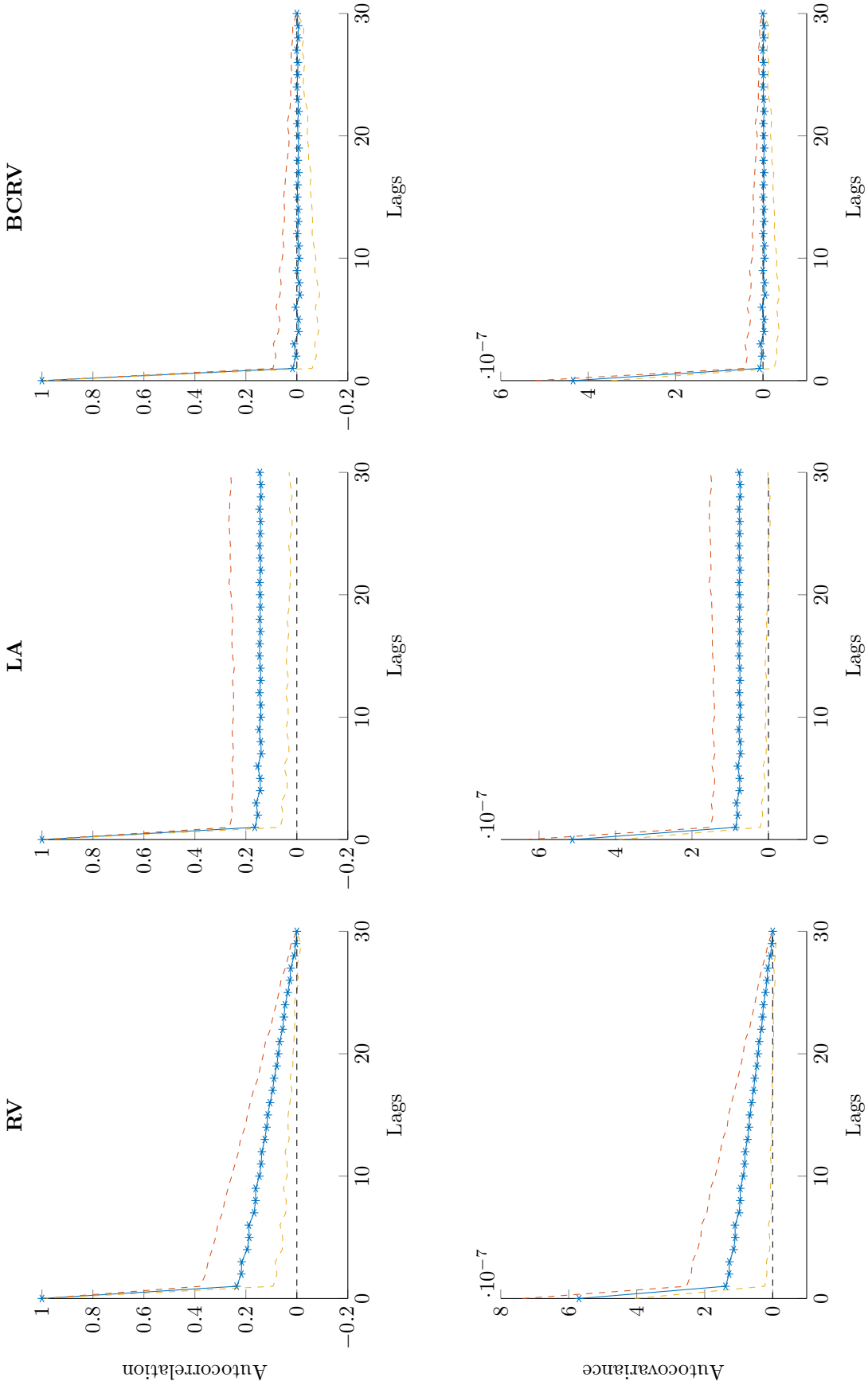


Figure 9: From the left to the right, we display the realized volatility (RV), local averaging (LA), and the bias corrected realized volatility (BCRV) estimators of the autocorrelations (top panel) and autocovariances (bottom panel) of noise against the number of lags j based on a subsample of the transaction data for Citigroup. Sample period: January, 2011. The subsample is recorded on a 1-sec time scale. The three estimators are applied to and next averaged over each of the 20 trading days. The stars indicate the means of the 20 estimates. The dashed lines are 2 standard deviations away from the mean. The tuning parameter of the RV estimator is $j_n = 30$.

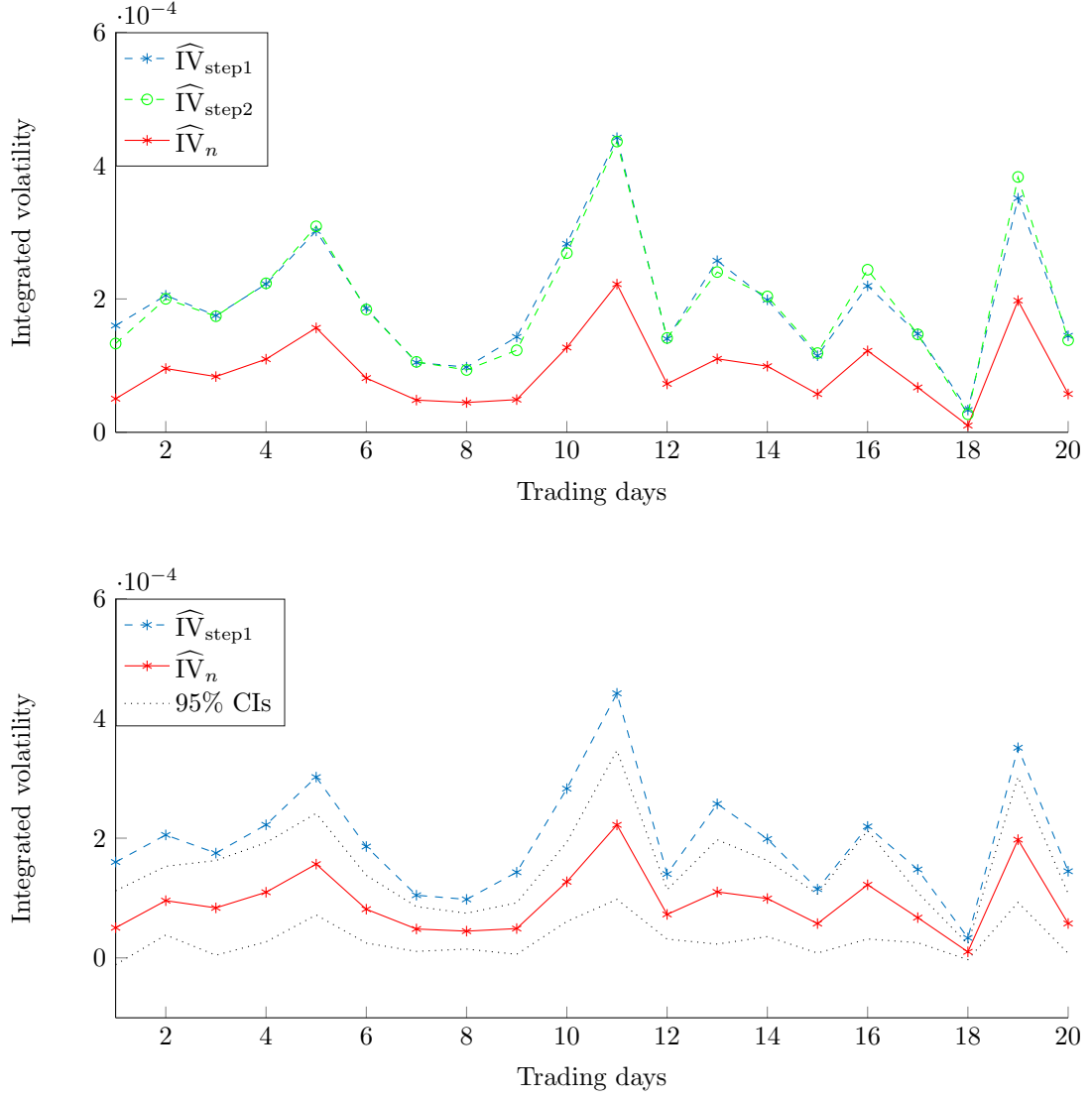


Figure 10: Estimation of the integrated volatility based on a subsample of the transaction data for Citigroup. Sample period: January, 2011, consisting of 20 trading days. The subsample is recorded on a 1-sec time scale. The estimators $\widehat{IV}_{\text{step1}}$, $\widehat{IV}_{\text{step2}}$, and \widehat{IV}_n are given by (28), (33), and (23). In the bottom panel, the asymptotic confidence intervals (CIs) are based on the limit distribution in Theorem 4.2. The tuning parameter of the RV estimator is $j_n = 30$ and $i_n = 5$.

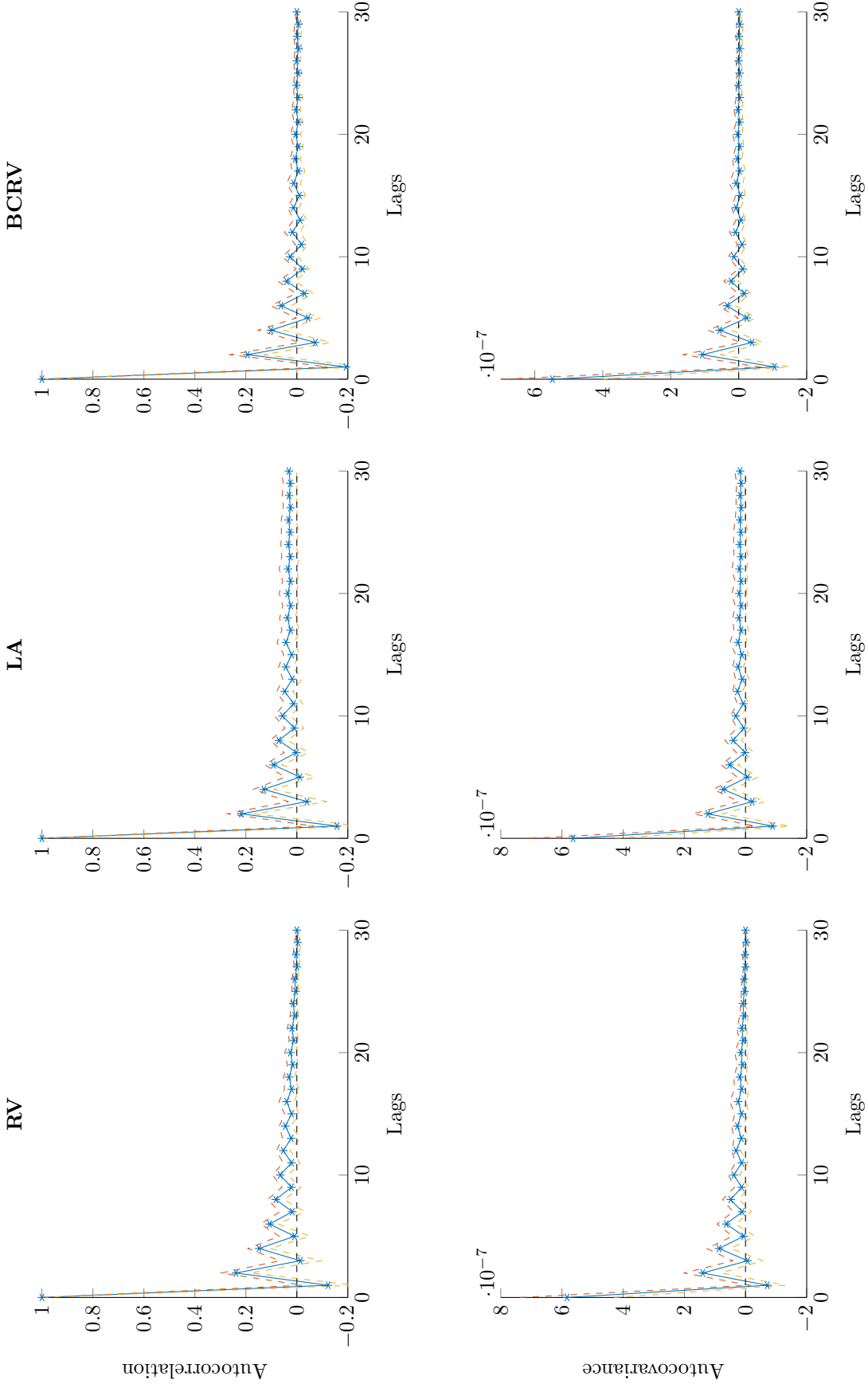


Figure 11: From the left to the right, we display the realized volatility (RV), local averaging (LA), and the bias corrected realized volatility (BCRV) estimators of the autocorrelations (top panel) and autocovariances (bottom panel) of noise against the number of lags j based on a subsample of the transaction data for Citigroup. Sample period: January, 2011. The subsample is recorded at tick time. On average there are 3.2 observations per second in the sample. The three estimators are applied to and next averaged over each of the 20 trading days. The stars indicate the means of the 20 estimates. The dashed lines are 2 standard deviations away from the mean. The tuning parameter of the RV estimator is $j_n = 30$.

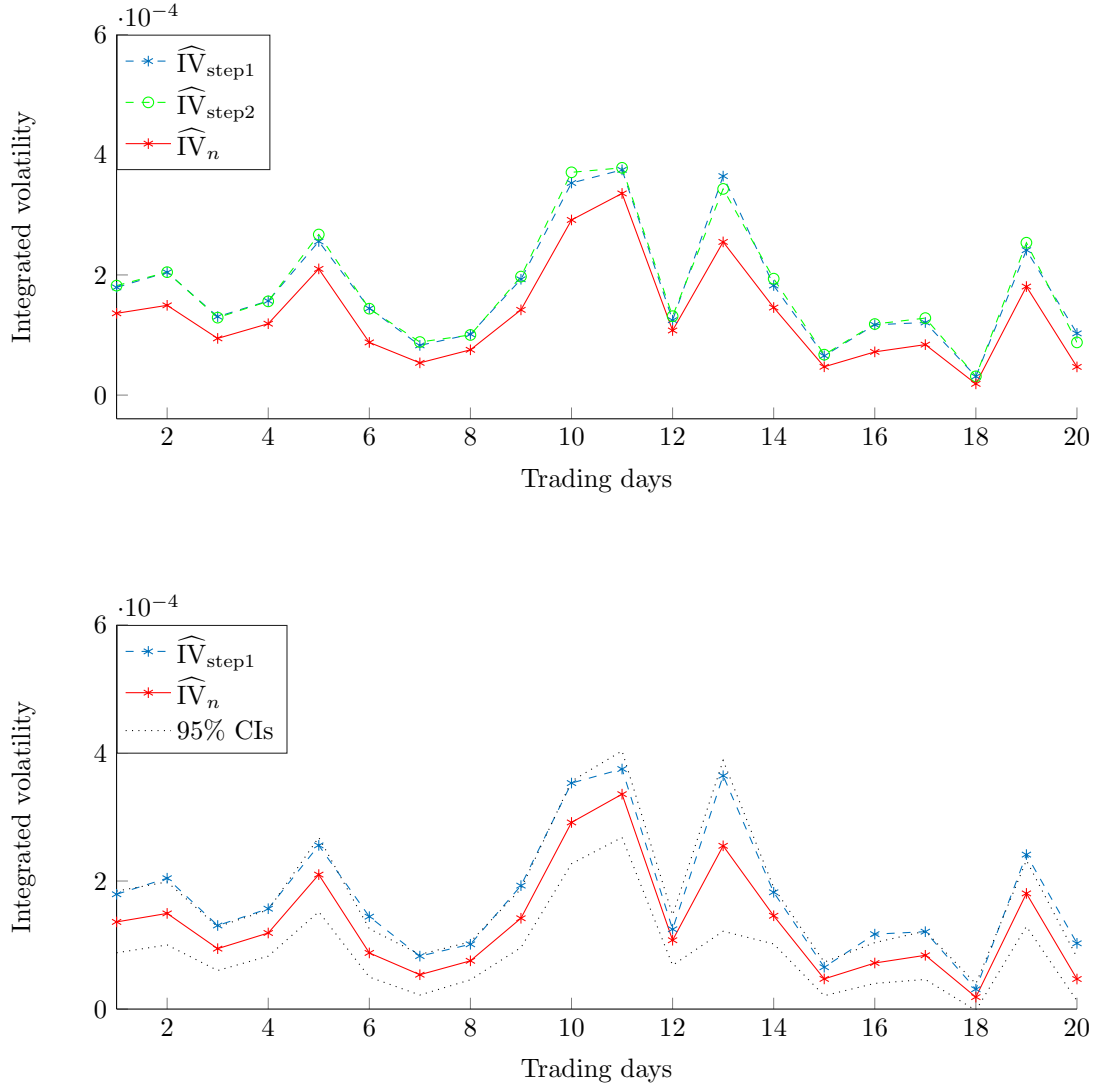


Figure 12: Estimation of the integrated volatility based on a subsample of the transaction data for Citigroup. Sample period: January, 2011, consisting of 20 trading days. The subsample is recorded at tick time. On average there are 3.2 observations per second in the sample. The estimators $\widehat{IV}_{\text{step1}}$, $\widehat{IV}_{\text{step2}}$, and \widehat{IV}_n are given by (28), (33), and (23). In the bottom panel, the asymptotic confidence intervals (CIs) are based on the limit distribution in Theorem 4.2. The tuning parameter of the RV estimator is $j_n = 30$ and $i_n = 10$.

Supplementary Material to
“Dependent Microstructure Noise and Integrated Volatility
Estimation from High-Frequency Data”

Appendix

Sections A–G in this appendix contain detailed technical proofs of our results. In Sections H and I, we provide additional Monte Carlo simulation and empirical results. In the proofs that follow the constants C and $\delta \in (0, 1)$ may vary from line to line. We add a subscript q if they depend on some parameter q .

A Proof of Proposition 3.1

Proof. Adopting the standard localization procedure (see e.g., Jacod and Protter (2011) for further details), we may assume that the processes a and σ are bounded by constants $C_a, C_\sigma > 0$. This yields for any such continuous Itô semimartingale X and stopping times $S \leq T$ that

$$\mathbb{E}(|X_T - X_S|^p | \mathcal{F}_S) \leq C_p \mathbb{E}(T - S | \mathcal{F}_S), \quad \forall p \geq 2. \quad (\text{A.1})$$

Let $\Delta_n = 1/n$. For any process V , we write $\Delta_{i,j}^n V := V_{i+j}^n - V_i^n$, $j = 1, 2, \dots, n - i$. Then, for the log-price process Y ,

$$[Y, Y]_n^j := \sum_{i=0}^{n-j} (\Delta_{i,j}^n Y)^2 = \sum_{i=0}^{n-j} (\Delta_{i,j}^n X)^2 + 2 \sum_{i=0}^{n-j} \Delta_{i,j}^n X \Delta_{i,j}^n U + \sum_{i=0}^{n-j} (\Delta_{i,j}^n U)^2. \quad (\text{A.2})$$

We now analyze the asymptotic properties of the three components on the right-hand side of (A.2):

- (i) First note that $\sum_{i=0}^{n-j} (\Delta_{i,j}^n X)^2 / j \xrightarrow{\mathbb{P}} [X, X]$, where $[X, X]$ is the quadratic variation of X .
- (ii) By the independence of X and U , we have

$$\sum_{i=0}^{n-j} \mathbb{E}((\Delta_{i,j}^n X \Delta_{i,j}^n U)^2) = \sum_{i=0}^{n-j} \mathbb{E}((\Delta_{i,j}^n X)^2) \mathbb{E}((\Delta_{i,j}^n U)^2) \leq Cj. \quad (\text{A.3})$$

The last inequality follows from the fact that U has bounded moments and from an application of (A.1). Next,

$$\begin{aligned} & \sum_{i, i': i < i'} \mathbb{E}(\Delta_{i,j}^n X \Delta_{i,j}^n U \Delta_{i',j}^n X \Delta_{i',j}^n U) \\ &= \sum_{i, i': i < i'} \mathbb{E}(\Delta_{i,j}^n X \Delta_{i',j}^n X) \mathbb{E}(\Delta_{i,j}^n U \Delta_{i',j}^n U) \\ &\leq Cj\Delta_n \left(\sum_{i, i': i+j < i'} \mathbb{E}(\Delta_{i,j}^n U \Delta_{i',j}^n U) + \sum_{i, i': i+j \geq i' > i} \mathbb{E}(\Delta_{i,j}^n U \Delta_{i',j}^n U) \right) \\ &\leq Cj^2. \end{aligned} \quad (\text{A.4})$$

The first inequality follows from the Cauchy-Schwarz inequality and (A.1). To see the second inequality, we apply the Cauchy-Schwarz inequality, Lemma VIII 3.102 of Jacod and Shiryaev (2003) (hereafter abbreviated as JS-Lemma), and the fact that $v > 2$ to obtain

$$\begin{aligned}
\sum_{i,i':i+j < i'} \mathbb{E}(\Delta_{i,j}^n U \Delta_{i',j}^n U) &= \sum_{i,i':i+j < i'} \mathbb{E}(\Delta_{i,j}^n U \mathbb{E}(\Delta_{i',j}^n U | \mathcal{F}_{(i+j)\Delta_n})) \\
&\leq C \sum_i \sum_{i':i+j < i'} \sqrt{\mathbb{E}\left(\left(\mathbb{E}(\Delta_{i',j}^n U | \mathcal{F}_{(i+j)\Delta_n})\right)^2\right)} \\
&\leq C \sum_i \sum_{i':i+j < i'} (i' - (i+j))^{-v/2} \leq C \Delta_n^{-1}.
\end{aligned} \tag{A.5}$$

Eqns. (A.3) and (A.4) imply that $\mathbb{E}\left(\left(\sum_{i=0}^{n-j} \Delta_{i,j}^n X \Delta_{i,j}^n U\right)^2\right) \leq Cj^2$, thus

$$\sum_{i=0}^{n-j} \Delta_{i,j}^n X \Delta_{i,j}^n U = O_p(j). \tag{A.6}$$

(iii) Turning to the last sum of (A.2), let $\nu_j := \mathbb{E}((U_{i+j}^n - U_i^n)^2) = 2(\mathbf{Var}(U) - \gamma(j))$. For $i > j$, we obtain the following in a similar way in which we derived (A.5):

$$|\mathbf{Cov}((U_j^n - U_0^n)^2, (U_{i+j}^n - U_i^n)^2)| \leq C(i-j)^{-v/2},$$

which implies

$$\mathbb{E}\left(\left(\sum_{i=0}^{n-j} ((\Delta_{i,j}^n U)^2 - \nu_j)\right)^2\right) \leq C \Delta_n^{-1} j. \tag{A.7}$$

For any fixed j , any j_n satisfying $\Delta_n j_n \rightarrow 0, j_n \rightarrow \infty$, we have by (A.6), (A.7) and (4) that

$$\begin{aligned}
\widehat{\langle Y, Y \rangle}_n(j) - (\mathbf{Var}(U) - \gamma(j)) &= O_p(\sqrt{\Delta_n j}); \\
\widehat{\langle Y, Y \rangle}_n(j_n) - \mathbf{Var}(U) &= O_p\left(\max\left\{\sqrt{\Delta_n j_n}, j_n^{-v/2}\right\}\right).
\end{aligned} \tag{A.8}$$

Now the stated results follow from (6).

□

B Proof of Proposition 3.2

Proof. Let $k = \lfloor \frac{n}{j} \rfloor$. We will adopt the square bracket notation in (A.2) for X and U as well. By Itô's isometry, we have

$$\begin{aligned}\mathbb{E}_\sigma([X, X]_{kj-1}^j) &= \sum_{i=0}^{j-1} \int_{i\Delta_n}^{((k-1)j+i)\Delta_n} \sigma_s^2 ds = \sum_{i=0}^{j-1} \left(\int_0^{kj\Delta_n} \sigma_s^2 ds - \int_0^{i\Delta_n} \sigma_s^2 ds - \int_{((k-1)j+i)\Delta_n}^{kj\Delta_n} \sigma_s^2 ds \right) \\ &= j \int_0^{kj\Delta_n} \sigma_s^2 ds + O_p(j^2 \Delta_n).\end{aligned}$$

Hence, we have

$$\mathbb{E}_\sigma([X, X]_n^j) = j \int_0^1 \sigma_s^2 ds + O_p(j^2 \Delta_n),$$

where the stochastic orders follow from the regularity conditions of the volatility path at 0 and 1. Furthermore, it is immediate that $\mathbb{E}_\sigma([U, U]_n^j) = 2(n-j+1)(\mathbf{Var}(U) - \gamma(j))$. Thus, we have, by the independence of X and U ,

$$\mathbb{E}_\sigma(\widehat{\langle Y, Y \rangle}_n(j)) = \frac{j \int_0^1 \sigma_s^2 ds}{2(n-j+1)} + \mathbf{Var}(U) - \gamma(j) + O_p(j^2 \Delta_n^2).$$

□

C Proof of Proposition 4.1

Proof of Proposition 4.1. Recall that

$$\begin{aligned}\bar{U}_m^n &= \frac{1}{k_n + 1} \sum_{i=(2m-2)k_n}^{(2m-1)k_n} (U_{i+k_n}^n - U_i^n) \\ &= \frac{1}{k_n + 1} \left(\sum_{i=(2m-1)k_n}^{2mk_n} U_i^n - \sum_{i=(2m-2)k_n}^{(2m-1)k_n} U_i^n \right).\end{aligned}$$

Also recall that U is symmetrically distributed around 0, whence \bar{U}_m^n is equal to the following in distribution:

$$\bar{U}_m^n \stackrel{d}{=} \frac{1}{k_n + 1} \left(\sum_{i=(2m-2)k_n}^{2mk_n} U_i^n \right) + O_p(\sqrt{\Delta_n}). \quad (\text{C.1})$$

Since $v > 2$, we have $\sigma_U^2 < \infty$, and an application of Corollary VIII 3.106 of [Jacod and Shiryaev \(2003\)](#) yields

$$\frac{1}{\sqrt{2k_n + 1}} \sum_{i=(2m-2)k_n}^{2mk_n} U_i^n \xrightarrow{\mathcal{L}} \mathcal{N}(0, \sigma_U^2),$$

whence

$$n^{1/4} \bar{U}_m^n \xrightarrow{\mathcal{L}} \mathcal{N}(0, 2\sigma_U^2/c).$$

□

D Proof of Proposition 4.2

Proof. For any fixed j , (A.8) implies $\widehat{\gamma(j)}_n - \gamma(j) = O_p\left(\max\left\{\sqrt{\Delta_n j_n}, j_n^{-v/2}\right\}\right)$. Therefore,

$$\widehat{\sigma_U^2} - \sum_{j=-i_n}^{i_n} \gamma(j) = O_p\left(\max\left\{\sqrt{\Delta_n j_n i_n^2}, j_n^{-v/2} i_n\right\}\right).$$

Now the result follows given that $\Delta_n j_n^3 \rightarrow 0, i_n \leq j_n, i_n \rightarrow \infty, v > 2$.

□

E Proof of Theorem 4.1

The proof of this theorem basically follows [Podolskij and Vetter \(2009b\)](#), but we need to deal with generally dependent noise.

First, we introduce some notation:

$$\beta_m^n := n^{1/4} \left(\sigma_{\frac{m-1}{M_n}} \bar{W}_m^n + \bar{U}_m^n \right); \quad (\text{E.1})$$

$$\xi_m^n := n^{1/4} \bar{Y}_m^n - \beta_m^n; \quad (\text{E.2})$$

$$\eta_m^n := \frac{n^{r/4}}{2c} \mathbb{E} \left(|\bar{Y}_m^n|^r \mid \mathcal{F}_{\frac{m-1}{M_n}} \right); \quad (\text{E.3})$$

$$\widetilde{\eta}_m^n := \frac{\mu_r}{2c} \left(\frac{2c}{3} \sigma_{\frac{m-1}{M_n}}^2 + \frac{2}{c} \sigma_U^2 \right)^{\frac{r}{2}}; \quad (\text{E.4})$$

$$\text{PAV}^n := \sum_{m=1}^{M_n} \eta_m^n; \quad (\text{E.5})$$

$$\widetilde{\text{PAV}}^n := \sum_{m=1}^{M_n} \widetilde{\eta}_m^n. \quad (\text{E.6})$$

Then, we state the following lemma:

Lemma E.1. For any $q > 0$, there is some constant $C_q > 0$ (depending on q), such that $\forall m$:

$$\mathbb{E}(|\xi_m^n|^q) + \mathbb{E}\left(\left|n^{1/4}\bar{X}_m^n\right|^q\right) < C_q; \quad (\text{E.7})$$

and the following holds for $q \in (0, 2r + \varepsilon)$ with ε as defined in Theorem 4.1:

$$\mathbb{E}(|\beta_m^n|^q) + \mathbb{E}\left(\left|n^{1/4}\bar{Y}_m^n\right|^q\right) < C_q. \quad (\text{E.8})$$

Proof of Lemma E.1. The boundedness of moments of ξ_m^n and $n^{1/4}\bar{X}_m^n$ (which don't depend on the noise) follows from Lemma 1 in Podolskij and Vetter (2009b).

Now we show the boundedness of $\mathbb{E}\left(\left|n^{1/4}\bar{Y}_m^n\right|^q\right)$ for $0 < q < 2r + \varepsilon$. We note (see Proposition 3.8 in White (2000)) that there is some C_q so that the following is true:

$$\mathbb{E}\left(\left|n^{1/4}\bar{Y}_m^n\right|^q\right) \leq C_q \left(\mathbb{E}\left(\left|n^{1/4}\bar{X}_m^n\right|^q\right) + \mathbb{E}\left(\left|n^{1/4}\bar{U}_m^n\right|^q\right) \right).$$

Boundedness of $\mathbb{E}\left(\left|n^{1/4}\bar{X}_m^n\right|^q\right)$ has already been established, while $\mathbb{E}\left(\left|n^{1/4}\bar{U}_m^n\right|^q\right)$ is bounded by Proposition 4.1 and a well known fact that convergence in distribution implies convergence in moments under uniformly bounded moments condition, see, e.g., Theorem 4.5.2 of Chung (2001). A similar proof holds for $\mathbb{E}(|\beta_m^n|^q)$. \square

Proof of Theorem 4.1. We present the proof in several steps.

(i) We first prove that

$$\text{PAV}(Y, r)_n - \frac{1}{M_n} \text{PAV}^n \xrightarrow{\mathbb{P}} 0. \quad (\text{E.9})$$

First, recall our choice of $M_n = \left\lfloor \frac{\sqrt{n}}{2c} \right\rfloor$. Next, observe that the difference on the left-hand side of (E.9) is in fact a sum of *martingale differences*:

$$\begin{aligned} & \text{PAV}(Y, r)_n - \frac{1}{M_n} \text{PAV}^n \\ &= \sum_{m=1}^{M_n} \frac{1}{\sqrt{n}} \left(\left|n^{\frac{1}{4}}\bar{Y}_m^n\right|^r - \mathbb{E}\left(\left|n^{\frac{1}{4}}\bar{Y}_m^n\right|^r \middle| \mathcal{F}_{\frac{m-1}{M_n}}\right) \right). \end{aligned}$$

In light of Lemma 2.2.11 in Jacod and Protter (2011), it suffices to show that

$$\frac{1}{n} \sum_{m=1}^{M_n} \mathbb{E}\left(\left|n^{\frac{1}{4}}\bar{Y}_m^n\right|^{2r} \middle| \mathcal{F}_{\frac{m-1}{M_n}}\right) \xrightarrow{\mathbb{P}} 0. \quad (\text{E.10})$$

But this follows from the boundedness established in Lemma E.1 and the choice of M_n .

(ii) Next, we prove that

$$\frac{1}{M_n} \text{PAV}^n - \frac{1}{M_n} \widetilde{\text{PAV}}^n \xrightarrow{\mathbb{P}} 0. \quad (\text{E.11})$$

To prove this, we proceed in several steps:

- (a) We first note that the error of approximating $n^{1/4} \bar{Y}_m^n$ by β_m^n , denoted by ξ_m^n in (E.2), is small in the sense that

$$\frac{1}{M_n} \sum_{m=1}^{M_n} \mathbb{E}(|\xi_m^n|^2) \rightarrow 0. \quad (\text{E.12})$$

For a detailed proof, see Podolskij and Vetter (2009b). (Note that our assumptions on the noise process are different from Podolskij and Vetter (2009b), but the noise terms don't appear in ξ_m^n .)

- (b) Next, define the approximation error

$$\zeta_m^n := \frac{|n^{1/4} \bar{Y}_m^n|^r - |\beta_m^n|^r}{2c}.$$

We note that this error is also small:

$$\frac{1}{M_n} \sum_{m=1}^{M_n} \mathbb{E}(|\zeta_m^n|) \rightarrow 0, \quad (\text{E.13})$$

which follows from

$$\frac{1}{M_n} \sum_{m=1}^{M_n} \mathbb{E}(|\zeta_m^n|^2) \rightarrow 0. \quad (\text{E.14})$$

This, in turn, can be proved following Podolskij and Vetter (2009b). (E.13) then follows, and it implies

$$\frac{1}{M_n} \sum_{m=1}^{M_n} \mathbb{E}(\zeta_m^n \mid \mathcal{F}_{\frac{m-1}{M_n}}) \xrightarrow{\mathbb{P}} 0, \quad (\text{E.15})$$

by the Markov inequality.

- (c) Now we show the following:

$$\mathbb{E}(|\beta_m^n|^r \mid \mathcal{F}_{\frac{m-1}{M_n}}) = \mu_r \left(\frac{2c}{3} \sigma_{\frac{m-1}{M_n}}^2 + \frac{2\sigma_U^2}{c} \right)^{\frac{r}{2}} + o_p(1), \quad (\text{E.16})$$

which holds uniformly in m . Recall that $r \geq 2$ is an even integer. Let $r_n \rightarrow \infty$ but $r_n = o(n^{1/2})$.

Denote

$$\begin{aligned}
\bar{\beta}_{m-1,r_n}^n &= \frac{n^{1/4}}{k_n + 1} \left(\sum_{i=(2m-2)k_n}^{(2m-2)k_n+r_n} \sigma_{\frac{m-1}{M_n}} (W_{i+k_n}^n - W_i^n) + (U_{i+k_n}^n - U_i^n) \right) \\
&=: n^{1/4} \left(\sigma_{\frac{m-1}{M_n}} \bar{W}_{m-1,r_n}^n + \bar{U}_{m-1,r_n}^n \right); \\
\bar{\beta}_{r_n,m}^n &= \frac{n^{1/4}}{k_n + 1} \left(\sum_{i=(2m-2)k_n+r_n+1}^{(2m-1)k_n} \sigma_{\frac{m-1}{M_n}} (W_{i+k_n}^n - W_i^n) + (U_{i+k_n}^n - U_i^n) \right) \\
&=: n^{1/4} \left(\sigma_{\frac{m-1}{M_n}} \bar{W}_{r_n,m}^n + \bar{U}_{r_n,m}^n \right).
\end{aligned}$$

Then, we have $\beta_m^n = \bar{\beta}_{m-1,r_n}^n + \bar{\beta}_{r_n,m}^n$. Furthermore, by our construction, $\bar{\beta}_{m-1,r_n}^n = o_p(1)$ and $\bar{\beta}_{r_n,m}^n$ has the same asymptotic distribution as β_m^n , which can be derived from the asymptotic distributions of $n^{1/4}\bar{U}_m^n$ and $n^{1/4}\bar{W}_m^n$, and the independence assumption between X and U .

By the Mean Value Theorem, we have

$$\mathbb{E} \left((\beta_m^n)^r - (\bar{\beta}_{r_n,m}^n)^r \middle| \mathcal{F}_{\frac{m-1}{M_n}} \right) = \mathbb{E} \left(r (\bar{\beta}_{r_n,m}^n)^{r-1} (\bar{\beta}_{m-1,r_n}^n) \middle| \mathcal{F}_{\frac{m-1}{M_n}} \right) + o_p(1).$$

The moment conditions and an application of Cauchy-Schwarz inequality yields

$$\mathbb{E} \left((\bar{\beta}_{r_n,m}^n)^{r-1} (\bar{\beta}_{m-1,r_n}^n) \middle| \mathcal{F}_{\frac{m-1}{M_n}} \right) = o_p(1).$$

Thus,

$$\mathbb{E} \left((\beta_m^n)^r \middle| \mathcal{F}_{\frac{m-1}{M_n}} \right) = \mathbb{E} \left((\bar{\beta}_{r_n,m}^n)^r \middle| \mathcal{F}_{\frac{m-1}{M_n}} \right) + o_p(1). \quad (\text{E.17})$$

For any $l \leq r$, define $\bar{U}_{r_n,m}^{n,l} := (n^{1/4}\bar{U}_{r_n,m}^n)^l$, and let

$$C_l := \mathbb{E} \left(\left(\mathbb{E} \left(\bar{U}_{r_n,m}^{n,l} \middle| \mathcal{F}_{\frac{m-1}{M_n}} \right) - \mathbb{E} \left(\bar{U}_{r_n,m}^{n,l} \right) \right)^2 \right).$$

By the JS-Lemma, we have $C_l \leq C r_n^{-v}$. Let

$$\Lambda_l := \frac{\mathbb{E} \left(\bar{U}_{r_n,m}^{n,l} \middle| \mathcal{F}_{\frac{m-1}{M_n}} \right) - \mathbb{E} \left(\bar{U}_{r_n,m}^{n,l} \right)}{\sqrt{C_l}};$$

note that $\mathbb{E}(\Lambda_l^2) = 1$. Thus,

$$\mathbb{E} \left(\bar{U}_{r_n,m}^{n,l} \middle| \mathcal{F}_{\frac{m-1}{M_n}} \right) = \mathbb{E} \left(\bar{U}_{r_n,m}^{n,l} \right) + \sqrt{C_l} \Lambda_l. \quad (\text{E.18})$$

Therefore, we can substitute the conditional moments by the unconditional moments and we

obtain the following ($C_r^k = \frac{r!}{k!(r-k)!}$ denotes the binomial coefficient):

$$\begin{aligned}
& \mathbb{E} \left(\left(\bar{\beta}_{r_n, m}^n \right)^r \middle| \mathcal{F}_{\frac{m-1}{M_n}} \right) \\
&= \mathbb{E} \left(\sum_{k=0}^r C_r^k \sigma_{\frac{m-1}{M_n}}^k \left(n^{1/4} \bar{W}_{r_n, m}^n \right)^k \left(n^{1/4} \bar{U}_{r_n, m}^n \right)^{r-k} \middle| \mathcal{F}_{\frac{m-1}{M_n}} \right) \\
&= \sum_{k=0}^r C_r^k \sigma_{\frac{m-1}{M_n}}^k \mathbb{E} \left(\left(n^{1/4} \bar{W}_{r_n, m}^n \right)^k \middle| \sigma_{\frac{m-1}{M_n}} \right) \mathbb{E} \left(\left(n^{1/4} \bar{U}_{r_n, m}^n \right)^{r-k} \middle| \mathcal{F}_{\frac{m-1}{M_n}} \right) \\
&= \mathbb{E} \left(\left(\bar{\beta}_{r_n, m}^n \right)^r \middle| \sigma_{\frac{m-1}{M_n}} \right) + \sum_{k=0}^r C_r^k \sigma_{\frac{m-1}{M_n}}^k \mathbb{E} \left(\left(n^{1/4} \bar{W}_{r_n, m}^n \right)^k \middle| \sigma_{\frac{m-1}{M_n}} \right) \sqrt{C_{r-k}} \Lambda_{r-k}.
\end{aligned}$$

Clearly, the last term is $o_p(1)$, and together with (E.17), we have

$$\begin{aligned}
\mathbb{E} \left(\left(\beta_m^n \right)^r \middle| \mathcal{F}_{\frac{m-1}{M_n}} \right) &= \mathbb{E} \left(\left(\bar{\beta}_{r_n, m}^n \right)^r \middle| \sigma_{\frac{m-1}{M_n}} \right) + o_p(1) \\
&= \mu_r \left(\frac{2c}{3} \sigma_{\frac{m-1}{M_n}}^2 + \frac{2\sigma_U^2}{c} \right)^{\frac{r}{2}} + o_p(1).
\end{aligned} \tag{E.19}$$

The last equality is a consequence of the asymptotic distribution of β_m^n .

(d) Now (E.11) follows from (E.15) and (E.19).

(iii) Following Proposition 2.2.8 in Jacod and Protter (2011), we see that the Riemann approximation converges:

$$\frac{1}{M_n} \sum_{m=1}^{M_n} \widetilde{\text{PAV}}^n \xrightarrow{\mathbb{P}} \text{PAV}(Y, r). \tag{E.20}$$

Recall that we already proved that

$$\text{PAV}(Y, r)_n - \frac{1}{M_n} \text{PAV}^n \xrightarrow{\mathbb{P}} 0; \quad \text{and} \quad \frac{1}{M_n} \text{PAV}^n - \frac{1}{M_n} \widetilde{\text{PAV}}^n \xrightarrow{\mathbb{P}} 0;$$

in previous steps. Now it is immediate to conclude that

$$\text{PAV}(Y, r)_n \xrightarrow{\mathbb{P}} \text{PAV}(Y, r).$$

This finalizes the proof of Theorem 4.1.

□

F Robustness to Irregular Sampling

In this section, we show that the consistency results for integrated volatility in Theorem 4.1 and Corollary 4.1 can be extended to irregular sampling times for the case $r = 2$, by adapting the approach in

Appendix C of Christensen et al. (2014) to allow for serially dependent noise in our general setting (recall $Y_i^n = X_{t_i^n} + U_i^n$). Let $f : [0, 1] \mapsto [0, 1]$ be a strictly increasing map with Lipschitz continuous first order derivatives. Let $f(0) = 0$ and $f(1) = 1$. Suppose that the observation times are $\{t_i^n = f(i/n) : 0 \leq i \leq n\}$. Let $C'_f = \max_{x \in [0, 1]} |f'(x)|$. Note that $C'_f < \infty$ by the continuity of f' .

First, we note that the asymptotic results related to the noise process we derived so far still hold under irregular sampling, because the noise is indexed by i rather than by t_i in our setting. The proof then proceeds in several steps:

1. We first provide the analogs of Lemma E.1 and step (i) in the proof of Theorem 4.1. Assume $q \geq 1$.

Then,

$$\begin{aligned}
\mathbb{E}(|\xi_m^n|^q) &= \mathbb{E} \left(\left| \frac{n^{1/4}}{k_n + 1} \sum_{i=(2m-2)k_n}^{(2m-1)k_n} X_{i+k_n}^n - X_i^n - \sigma_{t_{(2m-2)k_n}^n} (W_{i+k_n}^n - W_i^n) \right|^q \right) \\
&\leq \frac{n^{\frac{q}{4}}}{k_n + 1} \sum_{i=(2m-2)k_n}^{(2m-1)k_n} \mathbb{E} \left(\left| X_{i+k_n}^n - X_i^n - \sigma_{t_{(2m-2)k_n}^n} (W_{i+k_n}^n - W_i^n) \right|^q \right) \\
&= \frac{n^{\frac{q}{4}}}{k_n + 1} \sum_{i=(2m-2)k_n}^{(2m-1)k_n} \mathbb{E} \left(\left| \int_{t_i^n}^{t_{i+k_n}^n} (\alpha_s ds + (\sigma_s - \sigma_{t_{(2m-2)k_n}^n}) dW_s) \right|^q \right) \\
&\leq C_\alpha (C'_f)^q n^{-\frac{q}{4}} + \frac{C_q n^{\frac{q}{4}}}{k_n + 1} \sum_{i=(2m-2)k_n}^{(2m-1)k_n} \mathbb{E} \left(\left| \int_{t_i^n}^{t_{i+k_n}^n} (\sigma_s - \sigma_{t_{(2m-2)k_n}^n}) dW_s \right|^q \right) \\
&\leq C + \frac{C_q n^{\frac{q}{4}}}{k_n + 1} \sum_{i=(2m-2)k_n}^{(2m-1)k_n} \mathbb{E} \left(\left(\int_{t_i^n}^{t_{i+k_n}^n} |\sigma_s - \sigma_{t_{(2m-2)k_n}^n}|^2 ds \right)^{q/2} \right) \\
&\leq C.
\end{aligned}$$

The second inequality follows from the boundedness of α and C'_f . The third inequality is an application of the Burkholder-Davis-Gundy inequality. The last inequality follows from the fact that σ is bounded. Similarly, we can prove that $\mathbb{E}(|n^{1/4} \bar{X}_m^n|^q)$ is bounded. For $q \in (0, 1)$, the result is immediate using Jensen's inequality. Now the boundedness of $\mathbb{E}(|n^{1/4} \bar{Y}_m^n|^q)$, $q \in (0, 2r + \varepsilon)$, is obvious as the asymptotic distribution of the pre-averaged noise (which is indexed by i) does not change under irregular sampling.

2. Next, we prove the analog of step (ii) item (a) in the proof of Theorem 4.1. We have that

$$\begin{aligned}
& \mathbb{E}(|\xi_m^n|^2) \\
& \leq \sum_{i=(2m-2)k_n}^{(2m-1)k_n} \frac{\mathbb{E}\left(\left|n^{\frac{1}{4}}\left((X_{i+k_n}^n - X_i^n) - \sigma_{t_{(2m-2)k_n}^n}(W_{i+k_n}^n - W_i^n)\right)\right|^2\right)}{k_n + 1} \\
& = \sum_{i=(2m-2)k_n}^{(2m-1)k_n} \frac{\mathbb{E}\left(\left|n^{\frac{1}{4}}\left(\int_{t_i^n}^{t_{i+k_n}^n} \alpha_s ds + \int_{t_i^n}^{t_{i+k_n}^n} (\sigma_s - \sigma_{t_{(2m-2)k_n}^n}) dW_s\right)\right|^2\right)}{k_n + 1} \\
& \leq \sum_{i=(2m-2)k_n}^{(2m-1)k_n} \frac{2\mathbb{E}\left(n^{\frac{1}{2}}\left(\int_{t_i^n}^{t_{i+k_n}^n} \alpha_s ds\right)^2 + n^{1/2} \int_{t_i^n}^{t_{i+k_n}^n} (\sigma_s - \sigma_{t_{(2m-2)k_n}^n})^2 ds\right)}{k_n + 1} \\
& \leq \frac{C_f'^2 C_\alpha}{\sqrt{n}} + 2n^{1/2} \mathbb{E}\left(\int_{t_{(2m-2)k_n}^n}^{t_{2mk_n}^n} (\sigma_s - \sigma_{t_{(2m-2)k_n}^n})^2 ds\right).
\end{aligned}$$

The second inequality is due to the Cauchy's inequality and Itô's isometry. The third inequality is a consequence of the boundedness of $\alpha, |f'|$ and our choice of k_n ; it is obtained by taking i to be the lower and upper bound. Now we have

$$\begin{aligned}
\frac{1}{M_n} \sum_{m=1}^{M_n} \mathbb{E}(|\xi_m^n|^2) & \leq O(1/\sqrt{n}) + \frac{2n^{1/2}}{M_n} \sum_{m=1}^{M_n} \mathbb{E}\left(\int_{t_{(2m-2)k_n}^n}^{t_{2mk_n}^n} (\sigma_s - \sigma_{t_{(2m-2)k_n}^n})^2 ds\right) \\
& = O(1/\sqrt{n}) + 4c \int_0^1 \mathbb{E}\left((\sigma_s - \sigma_{\lfloor \frac{M_n s}{M_n} \rfloor})^2\right) ds.
\end{aligned}$$

Since $\sigma_{\lfloor \frac{M_n s}{M_n} \rfloor} \rightarrow \sigma_s$ -a.s., and σ is bounded, upon applying Lebesgue's Dominated Convergence Theorem, we obtain the analog of (E.12). We note that the analog of item (b) of step (ii) in the proof of Theorem 4.1 is directly obtained because (6.10) in Podolskij and Vetter (2009b) holds.

3. We now provide the analog of (E.19). First, we note that all the steps in proving (E.19) hold except those pertaining to the conditional variance of the pre-averaging Brownian motion. Next, we show that

$$\mathbf{Var}\left(n^{1/4} \overline{W}_m^n\right) = f'((2m-2)k_n/n) \frac{2c}{3} + o(1).$$

By the Lipschitz continuity of f' we obtain:

$$\begin{aligned}
& \text{Var} \left(\sum_{i=2(m-1)k_n}^{(2m-1)k_n} (W_{i+k_n}^n - W_i^n) \right) \\
&= \sum_{i=2(m-1)k_n}^{(2m-1)k_n} \text{Var}(W_{i+k_n}^n - W_i^n) + \sum_{i \neq j} \text{Cov}(W_{i+k_n}^n - W_i^n, W_{j+k_n}^n - W_j^n) \\
&= \sum_{i=2(m-2)k_n}^{(2m-1)k_n} (t_{i+k_n}^n - t_i^n) + 2 \sum_{i=(2m-2)k_n}^{(2m-1)k_n-1} \sum_{j>i} (t_{i+k_n}^n - t_j^n) \\
&= \sum_{i=(2m-2)k_n}^{(2m-1)k_n} \left(f'(i/n) \frac{k_n}{n} + o(k_n/n) \right) + 2 \sum_{i=(2m-2)k_n}^{(2m-1)k_n-1} \sum_{j>i} \left(f'(j/n) \frac{i+k_n-j}{n} + o(k_n/n) \right) \\
&= f' \left(\frac{(2m-2)k_n}{n} \right) \sum_{i=(2m-2)k_n}^{(2m-1)k_n} \left(\frac{k_n}{n} + o(k_n/n) \right) \\
&\quad + 2 \sum_{i=(2m-2)k_n}^{(2m-1)k_n-1} \sum_{j>i} \left(\frac{i+k_n-j}{n} + o(k_n/n) \right) \\
&= f' \left(\frac{(2m-2)k_n}{n} \right) \frac{2c^3 \sqrt{n}}{3} + o(\sqrt{n}).
\end{aligned}$$

Now the analog of (E.19) (with $r = 2$) is

$$\mathbb{E} \left((\beta_m^n)^2 \middle| \mathcal{F}_{t_{(2m-2)k_n}^n} \right) = \left(f' \left(\frac{(2m-2)k_n}{n} \right) \sigma_{f(\frac{(2m-2)k_n}{n})}^2 \frac{2c}{3} + \frac{2\sigma_U^2}{c} \right) + o_p(1). \quad (\text{F.1})$$

4. Finally, Riemann integrability yields the analog of (E.20):

$$\text{PAV}(Y, 2)_n \xrightarrow{\mathbb{P}} \int_0^1 \left(f'(s) \sigma_{f(s)}^2 \frac{2c}{3} + \frac{2\sigma_U^2}{c} \right) ds = \int_0^1 \left(\frac{2c}{3} \sigma_t^2 + \frac{2\sigma_U^2}{c} \right) dt.$$

The last equality is due to the change of variable $f(s) = t$.

G Proof of Theorem 4.2

We will first prove three lemmas. Then Theorem 4.2 follows as a consequence.

Lemma G.1. *We have that*

$$\mathbb{E} \left((\beta_m^n)^2 \middle| \mathcal{F}_{\frac{m-1}{M_n}} \right) = \left(\frac{2c}{3} \sigma_{\frac{m-1}{M_n}}^2 + \frac{2}{c} \sigma_U^2 \right) + o_p(n^{-1/4}). \quad (\text{G.1})$$

Proof. Let r_n satisfy

$$r_n \asymp n^\vartheta, \quad \frac{1}{4v} < \vartheta < \frac{1}{4}. \quad (\text{G.2})$$

To simplify notation, we let $s_m^n := (2m-2)k_n + r_n$, and we recall our earlier notation used in the proof of Theorem 4.1:

$$\begin{aligned}
\bar{\beta}_{m-1, r_n}^n &= \frac{n^{1/4}}{k_n + 1} \left(\sum_{i=(2m-2)k_n}^{(2m-2)k_n + r_n} \sigma_{\frac{m-1}{M_n}} (W_{i+k_n}^n - W_i^n) + (U_{i+k_n}^n - U_i^n) \right) \\
&=: n^{1/4} \left(\sigma_{\frac{m-1}{M_n}} \bar{W}_{m-1, r_n}^n + \bar{U}_{m-1, r_n}^n \right); \\
\bar{\beta}_{r_n, m}^n &= \frac{n^{1/4}}{k_n + 1} \left(\sum_{i=(2m-2)k_n + r_n + 1}^{(2m-1)k_n} \sigma_{\frac{m-1}{M_n}} (W_{i+k_n}^n - W_i^n) + (U_{i+k_n}^n - U_i^n) \right) \\
&=: n^{1/4} \left(\sigma_{\frac{m-1}{M_n}} \bar{W}_{r_n, m}^n + \bar{U}_{r_n, m}^n \right),
\end{aligned}$$

where $\bar{\beta}_{m-1, r_n}^n + \bar{\beta}_{r_n, m}^n = \beta_m^n$. The proof consists of three steps:

1. We start by showing that

$$\mathbb{E} \left((\beta_m^n)^2 \middle| \mathcal{F}_{\frac{m-1}{M_n}} \right) - \mathbb{E} \left((\bar{\beta}_{r_n, m}^n)^2 \middle| \mathcal{F}_{\frac{m-1}{M_n}} \right) = o_p(n^{-1/4}). \quad (\text{G.3})$$

To prove (G.3), we first prove that

$$\mathbb{E} \left((\bar{\beta}_{m-1, r_n}^n)^2 \middle| \mathcal{F}_{\frac{m-1}{M_n}} \right) = o_p(n^{-1/4}). \quad (\text{G.4})$$

For this purpose, we show the following for any $k \leq i < j$:

$$\mathbb{E} \left(\left| \mathbb{E} \left(U_i^n U_j^n \middle| \mathcal{F}_{\frac{k}{n}} \right) \right| \right) \leq C (j-i)^{-v/2}. \quad (\text{G.5})$$

To see this, we apply JS-Lemma to obtain that

$$c_{ij} := \mathbb{E} \left(\left(\mathbb{E} \left(U_j^n \middle| \mathcal{F}_{\frac{i}{n}} \right) \right)^2 \right) \leq C (j-i)^{-v}.$$

Then,

$$\mathbb{E} \left(\left| \mathbb{E} \left(U_i^n U_j^n \middle| \mathcal{F}_{\frac{k}{n}} \right) \right| \right) \leq \sqrt{C (j-i)^{-v}} \mathbb{E} \left(\left| \mathbb{E} \left(U_i^n \frac{\mathbb{E} \left(U_j^n \middle| \mathcal{F}_{\frac{i}{n}} \right)}{\sqrt{c_{ij}}} \middle| \mathcal{F}_{\frac{k}{n}} \right) \right| \right).$$

Now applying the Cauchy-Schwarz inequality and using the fact that the variance of noise is

bounded, we obtain (G.5). From (G.5) and some simple algebra we find that

$$\mathbb{E} \left(\left(\sum_{i=(2m-2)k_n}^{s_m^n} \sigma_{\frac{m-1}{M_n}} (W_{i+k_n}^n - W_i^n) \right)^2 \middle| \mathcal{F}_{\frac{m-1}{M_n}} \right)$$

is asymptotically much smaller than

$$\mathbb{E} \left(\left(\sum_{i=(2m-2)k_n}^{s_m^n} (U_{i+k_n}^n - U_i^n) \right)^2 \middle| \mathcal{F}_{\frac{m-1}{M_n}} \right) = O_p(r_n) = o_p(n^{1/4}), \quad (\text{G.6})$$

whence (G.4) holds.

Next, we prove that

$$\mathbb{E} \left(\left(\bar{\beta}_{r_n, m}^n \right) \left(\bar{\beta}_{m-1, r_n}^n \right) \middle| \mathcal{F}_{\frac{m-1}{M_n}} \right) = o_p(n^{-1/4}). \quad (\text{G.7})$$

(Note that the left-hand side of (G.3) is equal to the left-hand side of (G.4) plus twice the left-hand side of (G.7)). To show that

$$\frac{n^{1/2}}{(k_n + 1)^2} \mathbb{E} \left(\left(\sum_{i=(2m-2)k_n}^{s_m^n} U_{i+k_n}^n - U_i^n \right) \left(\sum_{i=s_m^n+1}^{(2m-1)k_n} U_{i+k_n}^n - U_i^n \right) \middle| \mathcal{F}_{\frac{m-1}{M_n}} \right) = o_p(n^{-1/4}),$$

we first evaluate

$$\begin{aligned} & \frac{n^{1/2}}{(k_n + 1)^2} \left| \mathbb{E} \left(\left(\sum_{i=(2m-2)k_n}^{s_m^n} U_{i+k_n}^n \right) \left(\sum_{j=s_m^n+1}^{(2m-1)k_n} U_{j+k_n}^n \right) \middle| \mathcal{F}_{\frac{m-1}{M_n}} \right) \right| \\ & \leq \frac{n^{1/2}}{(k_n + 1)^2} \sum_{i=(2m-2)k_n}^{s_m^n} \sum_{j=s_m^n+1}^{(2m-1)k_n} \left| \mathbb{E} \left(U_{i+k_n}^n U_{j+k_n}^n \middle| \mathcal{F}_{\frac{m-1}{M_n}} \right) \right|. \end{aligned}$$

Now apply (G.5) and by the fact that $v > 4$, we have

$$\begin{aligned} \sum_{i=(2m-2)k_n}^{s_m^n} \sum_{j=s_m^n+1}^{(2m-1)k_n} \mathbb{E} \left(\left| \mathbb{E} \left(U_{i+k_n}^n U_{j+k_n}^n \middle| \mathcal{F}_{\frac{m-1}{M_n}} \right) \right| \right) & \stackrel{(\text{G.5})}{\leq} \sum_{i=(2m-2)k_n}^{s_m^n} \sum_{j=s_m^n+1}^{(2m-1)k_n} C(j-i)^{-v/2} \\ & \leq C \sum_{\ell=1}^{r_n} \ell^{1-\frac{v}{2}} \leq C. \end{aligned}$$

Similarly, we can prove that the other three cross products have the same order. It is also easy to verify that

$$\frac{\sqrt{n}}{(k_n + 1)^2} \mathbb{E} \left(\sum_{i=(2m-2)k_n}^{s_m^n} (W_{i+k_n}^n - W_i^n) \sum_{j=s_m^n+1}^{(2m-1)k_n} (W_{j+k_n}^n - W_j^n) \right) = O(r_n/\sqrt{n}).$$

Now (G.7) is proved and consequently (G.3) follows from (G.4) and (G.7).

2. Next, we prove that

$$\mathbb{E} \left(\left(\bar{\beta}_{r_n, m}^n \right)^2 \middle| \mathcal{F}_{\frac{m-1}{M_n}} \right) - \mathbb{E} \left(\left(\bar{\beta}_{r_n, m}^n \right)^2 \middle| \sigma_{\frac{m-1}{M_n}} \right) = o_p(n^{-1/4}). \quad (\text{G.8})$$

For this purpose, we note that

$$\begin{aligned} & \frac{(k_n + 1)^2}{\sqrt{n}} \left| \mathbb{E} \left(\left(\bar{\beta}_{r_n, m}^n \right)^2 \middle| \mathcal{F}_{\frac{m-1}{M_n}} \right) - \mathbb{E} \left(\left(\bar{\beta}_{r_n, m}^n \right)^2 \middle| \sigma_{\frac{m-1}{M_n}} \right) \right| \\ &= \left| \mathbb{E} \left(\left(\sum_{i=s_m^n+1}^{(2m-1)k_n} (U_{i+k_n}^n - U_i^n) \right)^2 \middle| \mathcal{F}_{\frac{m-1}{M_n}} \right) - \mathbb{E} \left(\left(\sum_{i=s_m^n+1}^{(2m-1)k_n} (U_{i+k_n}^n - U_i^n) \right)^2 \right) \right|. \end{aligned}$$

Applying again the JS-Lemma, we find that

$$\mathbb{E} \left(\left(\bar{\beta}_{r_n, m}^n \right)^2 \middle| \mathcal{F}_{\frac{m-1}{M_n}} \right) - \mathbb{E} \left(\left(\bar{\beta}_{r_n, m}^n \right)^2 \middle| \sigma_{\frac{m-1}{M_n}} \right) = O_p(r_n^{-v}),$$

whence (G.8) follows from (G.2).

3. Finally, we show that

$$\mathbb{E} \left(\left(\bar{\beta}_{r_n, m}^n \right)^2 \middle| \sigma_{\frac{m-1}{M_n}} \right) = \left(\frac{2c}{3} \sigma_{\frac{m-1}{M_n}}^2 + \frac{2}{c} \sigma_U^2 \right) + o_p(n^{-1/4}). \quad (\text{G.9})$$

This follows from the following equalities, which are straightforward:

$$\mathbb{E} \left(\left(\frac{n^{1/4}}{k_n + 1} \left(\sum_{i=s_m^n+1}^{(2m-1)k_n} \sigma_{\frac{m-1}{M_n}} (W_{i+k_n}^n - W_i^n) \right) \right)^2 \middle| \sigma_{\frac{m-1}{M_n}} \right) = \frac{2c}{3} \sigma_{\frac{m-1}{M_n}}^2 + o_p(n^{-1/4}),$$

$$\mathbb{E} \left(\left(\frac{n^{1/4}}{k_n + 1} \left(\sum_{i=s_m^n+1}^{(2m-1)k_n} (U_{i+k_n}^n - U_i^n) \right) \right)^2 \middle| \sigma_{\frac{m-1}{M_n}} \right) = \frac{2\sigma_U^2}{c} + o_p(n^{-1/4}).$$

Now (G.1) follows from (G.3), (G.8) and (G.9), and the proof is complete. \square

Lemma G.2. *Let*

$$L_n := n^{-1/4} \sum_{m=1}^{M_n} \left((\beta_m^n)^2 - \mathbb{E} \left((\beta_m^n)^2 \middle| \mathcal{F}_{\frac{m-1}{M_n}} \right) \right).$$

Then, we have the following stable convergence in law:

$$L_n \xrightarrow{\mathcal{L}-s} \sqrt{\frac{1}{c}} \int_0^1 \left(\frac{2c}{3} \sigma_s^2 + \frac{2\sigma_U^2}{c} \right) dW'_s, \quad (\text{G.10})$$

where W' is a standard Wiener process independent of \mathcal{F} .

Proof. Let $\theta_m^n := n^{-1/4} \left((\beta_m^n)^2 - \left(\frac{2c}{3} \sigma_{\frac{m-1}{M_n}}^2 + \frac{2}{c} \sigma_U^2 \right) \right)$. Then,

$$L_n = \sum_{m=1}^{M_n} \theta_m^n + o_p(1),$$

by Lemma G.1. We also have

$$\sum_{m=1}^{M_n} \mathbb{E} \left(\theta_m^n \middle| \mathcal{F}_{\frac{m-1}{M_n}} \right) \xrightarrow{\mathbb{P}} 0, \quad (\text{G.11})$$

again by Lemma G.1 and

$$\begin{aligned} \sum_{m=1}^{M_n} \mathbb{E} \left((\theta_m^n)^2 \middle| \mathcal{F}_{\frac{m-1}{M_n}} \right) &= \frac{1}{2cM_n} \sum_{m=1}^{M_n} \mathbb{E} \left((\beta_m^n)^4 \middle| \mathcal{F}_{\frac{m-1}{M_n}} \right) + \frac{1}{2cM_n} \sum_{m=1}^{M_n} \left(\frac{2c}{3} \sigma_{\frac{m-1}{M_n}}^2 + \frac{2\sigma_U^2}{c} \right)^2 \\ &\quad - \frac{1}{cM_n} \sum_{m=1}^{M_n} \mathbb{E} \left((\beta_m^n)^2 \middle| \mathcal{F}_{\frac{m-1}{M_n}} \right) \left(\frac{2c}{3} \sigma_{\frac{m-1}{M_n}}^2 + \frac{2\sigma_U^2}{c} \right). \end{aligned}$$

Now it follows from (E.16) and a Riemann approximation that

$$\sum_{m=1}^{M_n} \mathbb{E} \left((\theta_m^n)^2 \middle| \mathcal{F}_{\frac{m-1}{M_n}} \right) \xrightarrow{\mathbb{P}} \frac{1}{c} \int_0^1 \left(\frac{2c}{3} \sigma_u^2 + \frac{2\sigma_U^2}{c} \right)^2 du. \quad (\text{G.12})$$

Next, denote $\overline{\Delta_m^n V} = V_{(2m-1)k_n}^n - V_{2(m-1)k_n}^n$, for any process V . We will show that

$$\sum_{m=1}^{M_n} \mathbb{E} \left(\theta_m^n \overline{\Delta_m^n N} \middle| \mathcal{F}_{2(m-1)k_n}^n \right) \xrightarrow{\mathbb{P}} 0, \quad (\text{G.13})$$

for any bounded martingale N defined on the same probability space, where $\mathcal{F}_i^n = \mathcal{F}_{i/n}$ whence $\mathcal{F}_{2(m-1)k_n}^n = \mathcal{F}_{\frac{m-1}{M_n}}^n$. To complete the proof, it is convenient to specify the respective probability spaces as follows. (We can always extend the probability space — whether the noise process and the efficient price process are defined on the same probability space or not — see e.g., the detailed arguments in [Jacod et al. \(2017b\)](#).) The efficient price process lives on $(\Omega', \mathcal{F}', (\mathcal{F}'_t)_{t \in \mathbb{R}}, \mathbb{P}')$. The noise process $(U_i)_{i \in \mathbb{N}}$ is defined on $(\Omega'', \mathcal{F}'', (\mathcal{F}''_i)_{i \in \mathbb{N}}, \mathbb{P}'')$, where the filtration is defined by $\mathcal{F}''_i = \sigma(U_j, j \leq i, j \in \mathbb{N})$ and $\mathcal{F}'' = \bigvee_{i \in \mathbb{N}} \mathcal{F}''_i$.

Let

$$\Omega = \Omega' \times \Omega'', \quad \mathcal{F} = \mathcal{F}' \otimes \mathcal{F}'', \quad \mathbb{P}(\mathrm{d}\omega', \mathrm{d}\omega'') = \mathbb{P}'(\mathrm{d}\omega') \mathbb{P}''(\mathrm{d}\omega''). \quad (\text{G.14})$$

For a realization of observation times $(t_i^n)_{0 \leq i \leq n}$, we introduce $\mathcal{F}_i^n = \mathcal{F}'_{t_i^n} \otimes \mathcal{F}''_i$.

According to [Jacod et al. \(2009\)](#) and the proof of Theorem IX 7.28 of [Jacod and Shiryaev \(2003\)](#) it suffices to consider martingales in \mathcal{N}^0 or \mathcal{N}^1 , where \mathcal{N}^0 is the set of all bounded martingales on $(\Omega', \mathcal{F}', \mathbb{P}')$, orthogonal to W , and \mathcal{N}^1 is the set of all martingales having a limit $N_\infty = f(Y_{t_1}, \dots, Y_{t_q})$, where f is any bounded Borel function on \mathbb{R}^q , $t_1 < \dots < t_q$ and $q \geq 1$.

First, let $N \in \mathcal{N}^0$ and let $\tilde{\mathcal{F}}'_t = \bigcap_{s>t} \mathcal{F}'_s \otimes \mathcal{F}''$. Then, for any $t > \frac{m-1}{M_n}$, $\bar{\theta}_m^n(t) := \mathbb{E}\left(\theta_m^n \middle| \tilde{\mathcal{F}}'_t\right)$, conditional on $\sigma_{\frac{m-1}{M_n}}$, is a martingale with respect to the filtration generated by $\{W_t - W_{\frac{m-1}{M_n}} \mid t > \frac{m-1}{M_n}\}$. By the martingale representation theorem, we have $\bar{\theta}_m^n(t) = \bar{\theta}_m^n(\frac{m-1}{M_n}) + \int_{\frac{m-1}{M_n}}^t \gamma_u \mathrm{d}W_u$ for some predictable process γ . Now it follows from the orthogonality of W, N and the martingale property of N that

$$\mathbb{E}\left(\theta_m^n \bar{\Delta}_m^n N \middle| \tilde{\mathcal{F}}'_{\frac{m-1}{M_n}}\right) = \mathbb{E}\left(\left(\theta_m^n - \bar{\theta}_m^n\left(\frac{m-1}{M_n}\right)\right) \bar{\Delta}_m^n N + \bar{\theta}_m^n\left(\frac{m-1}{M_n}\right) \bar{\Delta}_m^n N \middle| \tilde{\mathcal{F}}'_{\frac{m-1}{M_n}}\right) = 0,$$

which leads to

$$\mathbb{E}\left(\theta_m^n \bar{\Delta}_m^n N \middle| \mathcal{F}_{2(m-1)k_n}^n\right) = 0, \quad (\text{G.15})$$

since $\mathcal{F}_t \subset \tilde{\mathcal{F}}'_t$.

Next, assume that $N \in \mathcal{N}^1$. It can be shown (see [Jacod et al. \(2009\)](#)) that there exists some \hat{f}_t such that $t \in [t_l, t_{l+1})$, $N_t = \hat{f}_t(Y_{t_0}, Y_{t_1}, \dots, Y_{t_l})$ with $t_0 = 0, t_{q+1} = \infty$, and such that it is measurable in $(Y_{t_1}, \dots, Y_{t_l})$. Hence, $\bar{\Delta}_m^n N = 0$ if it does not cover any of the points t_1, \dots, t_{q+1} . But such intervals (to compute $\bar{\Delta}_m^n N$) that contain any of t_1, \dots, t_{q+1} are at most finite in number. Furthermore, by the boundedness of N and the conditional Cauchy-Schwarz inequality, we have the following:

$$\mathbb{E}\left(|\theta_m^n \bar{\Delta}_m^n N| \middle| \mathcal{F}_{2(m-1)k_n}^n\right) \leq \sqrt{\mathbb{E}\left((\theta_m^n)^2 \middle| \mathcal{F}_{2(m-1)k_n}^n\right)} \sqrt{\mathbb{E}\left((\bar{\Delta}_m^n N)^2 \middle| \mathcal{F}_{2(m-1)k_n}^n\right)} = O_p(n^{-1/4}).$$

Now [\(G.13\)](#) follows since there are at most finitely many such intervals.

The following is also trivial:

$$\mathbb{E}\left(\theta_m^n \bar{\Delta}_m^n W \middle| \mathcal{F}_{2(m-1)k_n}^n\right) = 0, \quad (\text{G.16})$$

since θ_m^n is an even functional of U and W and (U, W) are distributed symmetrically.

From (E.19), we know that $(\theta_m^n)^2 \mathbf{1}_{\{|\theta_m^n| > \varepsilon\}} = o_p(n^{-1/2})$ for any $\varepsilon > 0$. We then have

$$\sum_{m=1}^{M_n} \mathbb{E} \left((\theta_m^n)^2 \mathbf{1}_{\{|\theta_m^n| > \varepsilon\}} \middle| \mathcal{F}_{2(m-1)k_n}^n \right) \xrightarrow{\mathbb{P}} 0. \quad (\text{G.17})$$

Now the proof is complete in view of (G.11), (G.12), (G.13), (G.16) and (G.17), and Theorem IX 7.28 of Jacod and Shiryaev (2003). \square

Lemma G.3. *We have that*

$$\sum_{m=1}^{M_n} (\bar{Y}_m^n)^2 - \frac{1}{\sqrt{n}} \sum_{m=1}^{M_n} (\beta_m^n)^2 = o_p(n^{-1/4}). \quad (\text{G.18})$$

Proof. Denote

$$\tilde{Y}_m^n = \sigma_{\frac{m-1}{M_n}} \bar{W}_m^n + \bar{U}_m^n. \quad (\text{G.19})$$

Then,

$$\mathbb{E} \left(\left| \sum_{m=1}^{M_n} (\bar{Y}_m^n)^2 - \frac{1}{\sqrt{n}} \sum_{m=1}^{M_n} (\beta_m^n)^2 \right| \right) \leq \sum_{m=1}^{M_n} \sqrt{\mathbb{E} \left((\bar{Y}_m^n - \tilde{Y}_m^n)^2 \right)} \sqrt{\mathbb{E} \left((\bar{Y}_m^n + \tilde{Y}_m^n)^2 \right)}.$$

Since $\sqrt{\mathbb{E} \left((\bar{Y}_m^n + \tilde{Y}_m^n)^2 \right)} = O(n^{-1/4})$, the result follows if

$$\sum_{m=1}^{M_n} \sqrt{\mathbb{E} \left((\bar{Y}_m^n - \tilde{Y}_m^n)^2 \right)} \rightarrow 0. \quad (\text{G.20})$$

But this follows directly from Lemma 7.8 in Barndorff-Nielsen et al. (2006). \square

Proof of Theorem 4.2. Now the proof of Theorem 4.2 is complete in view of (G.10) and (G.18), and our consistency result in (22). \square

H Simulation Study under Stochastic Volatility

In this section, we provide additional simulation results in the presence of stochastic volatility. We simulate the microstructure noise process employing various combinations of dependence structure and sampling frequency.

We assume that the efficient log-price is generated by the following dynamics:

$$dX_t = -\delta(X_t - \mu_1)dt + \sigma_t dW_t, \quad d\sigma_t^2 = \kappa(\mu_2 - \sigma_t^2)dt + \gamma\sigma_t dB_t,$$

where B is a standard Brownian motion and its quadratic covariation with the standard Brownian motion W is ϱt . We set the parameters as follows: $\delta = 0.5$, $\mu_1 = 1.6$, $\kappa = 5/252$, $\mu_2 = 0.04/252$, $\gamma = 0.05/252$, and $\varrho = -0.5$. We employ the same noise process as in (34). We set $\mathbb{E}(V^2) = 1.9 \times 10^{-7}$, and $\mathbb{E}(\epsilon^2) = 1.3 \times 10^{-7}$. Note that these parameters are slightly different from those in Section 6, which were based on Ait-Sahalia et al. (2011). They are chosen to mimic the results of our empirical studies.

Figure H.13 presents the estimates of the second moments of noise. Clearly, the bias correction can be important, potentially yielding significantly improved results. Turning to the estimation of the integrated volatility using $\widehat{IV}_{\text{step1}}$, \widehat{IV}_n , $\widehat{IV}_{\text{step2}}$ and $\widehat{IV}_{\text{step3}}$, we observe from Table H.3 similar results under stochastic volatility as in our previous simulation studies that assumed deterministic volatility: the two-step estimators of the integrated volatility have much smaller bias and only slightly larger standard deviations when noise is dependent. One more iteration of bias corrections further improves the performance when noise is serially correlated. They also deliver reliable estimates when noise turns out to be independent.

ρ, Δ_n	$\rho = 0.7, \Delta_n = 0.2 \text{ sec}$	$\rho = 0, \Delta_n = 1 \text{ sec}$	$\rho = -0.7, \Delta_n = 0.4 \text{ sec}$
$\widehat{IV}_{\text{step1}} - \int_0^1 \sigma_t^2 dt$	5.02e-5 (1.10e-5)	4.33e-7 (1.32e-5)	-1.50e-5 (9.97e-6)
$\widehat{IV}_n - \int_0^1 \sigma_t^2 dt$	-1.64e-5 (1.09e-5)	-7.82e-5 (1.18e-5)	-3.17e-5 (9.77e-6)
$\widehat{IV}_{\text{step2}} - \int_0^1 \sigma_t^2 dt$	4.32e-6 (1.20e-5)	9.94e-7 (1.79e-5)	-3.15e-6 (1.17e-5)
$\widehat{IV}_{\text{step3}} - \int_0^1 \sigma_t^2 dt$	-2.32e-7 (1.21e-5)	1.27e-6 (2.06e-5)	-8.05e-7 (1.21e-5)

Table H.3: Estimation of the integrated volatility in the presence of stochastic volatility and under various combinations of noise dependence structure and sampling frequency. We report the means of the bias of the four integrated volatility estimators: $\widehat{IV}_{\text{step1}} - \int_0^1 \sigma_t^2 dt$, $\widehat{IV}_n - \int_0^1 \sigma_t^2 dt$, $\widehat{IV}_{\text{step2}} - \int_0^1 \sigma_t^2 dt$ and $\widehat{IV}_{\text{step3}} - \int_0^1 \sigma_t^2 dt$, based on 1,000 simulations with standard deviations between parentheses. From the left to the right, the three combinations of ρ, Δ_n mimic transaction time sampling, regular time sampling (at 1 sec scale), and tick time sampling. The tuning parameters are set as follows: $j_n = 20$, $i_n = 10$ and $c = 0.2$.

I Empirical Study of Transaction Data for General Electric

We collect 2,721,475 transaction prices of General Electric (GE) over the month January 2011. On average there are 5.8 observations per second. In contrast to the analysis of Citigroup transaction prices in Sections 7.2 and 7.3, bias correction plays a very pronounced role here. Despite the high data frequency, the finite sample bias can be very significant if the underlying noise-to-signal ratio is small (recall Remark 3.3). This is indeed the case as Figure I.1 reveals: compared with Citigroup, the data frequency of the General Electric sample is typically lower but the noise-to-signal ratio is also (much) smaller. While the data frequency is immediately available, the noise-to-signal ratio is latent. Therefore, one should always be wary to rely solely on asymptotic theory in practice.

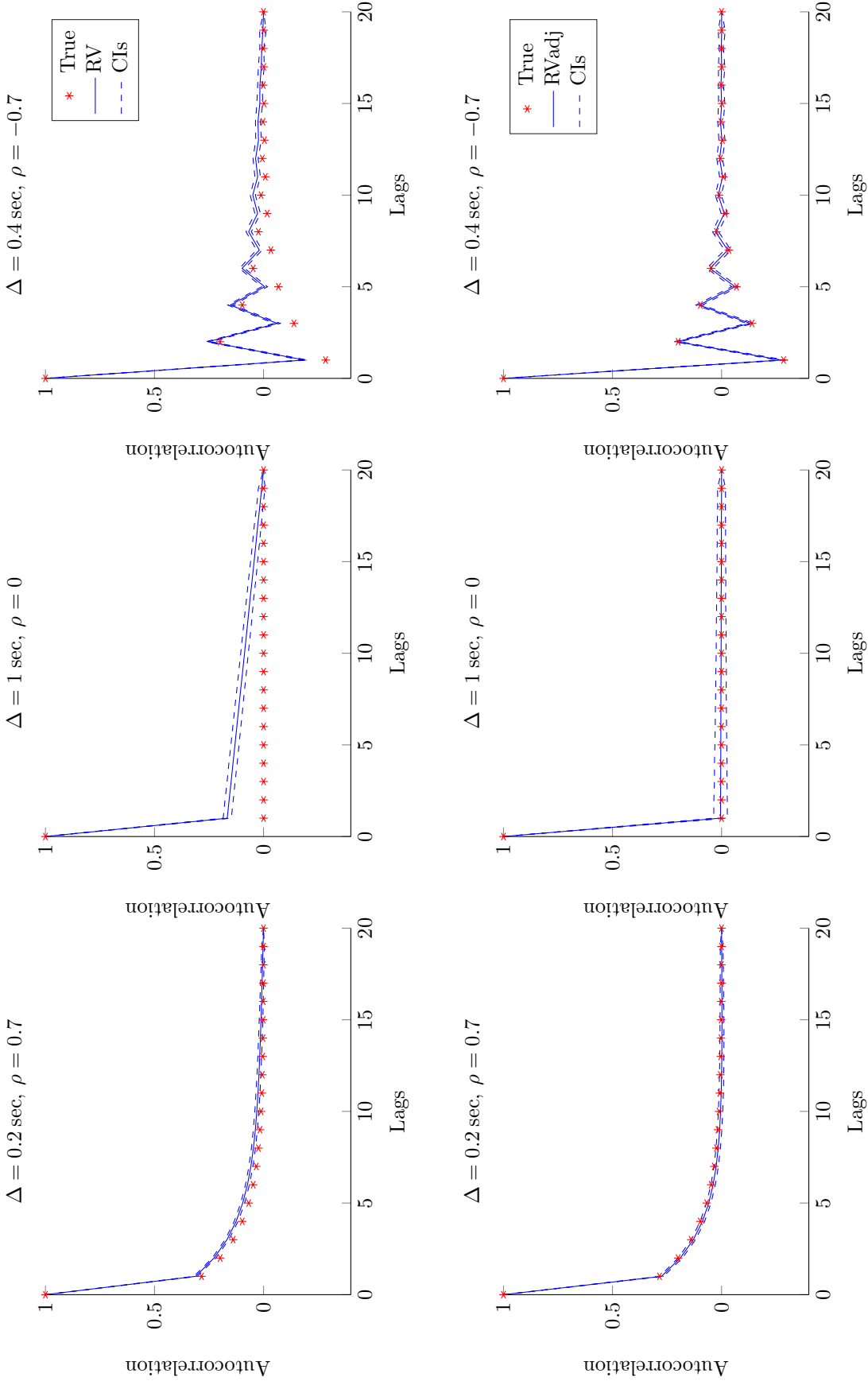


Figure H.13: Realized volatility (RV) and bias corrected realized volatility (RVadj) estimators of the autocorrelations of noise in the presence of stochastic volatility against the number of lags j , averaged over 1,000 simulated samples. Top panel: RV estimators of the autocorrelations of noise (solid). Bottom panel: RV estimators of the autocorrelations of noise with finite sample bias correction (solid). The true autocorrelations are displayed in stars and the 95% simulated confidence intervals are dashed. From the left to the right, the three combinations of ρ, Δ_n mimic transaction time sampling, regular time sampling (at 1 sec scale), and tick time sampling. The tuning parameters are set as follows: $j_n = 20$, $i_n = 10$ and $c = 0.2$.

The top panel of Figure I.2 shows that both the realized volatility (RV) and local averaging (LA) estimators indicate that the noise is strongly autocorrelated, while the bias corrected realized volatility (BCRV) estimator reveals that the noise is only weakly dependent. Such a pattern also appears in our simulation study, where we have seen that it is the finite sample bias that induces this discrepancy. The bottom panel of Figure I.2 plots two estimators of the integrated volatility, \widehat{IV}_n and $\widehat{IV}_{\text{step2}}$, to illustrate that the finite sample bias correction is particularly essential. If one would solely rely on asymptotic theory, then one would end up with much lower estimates and narrow confidence intervals that may well exclude the true values!

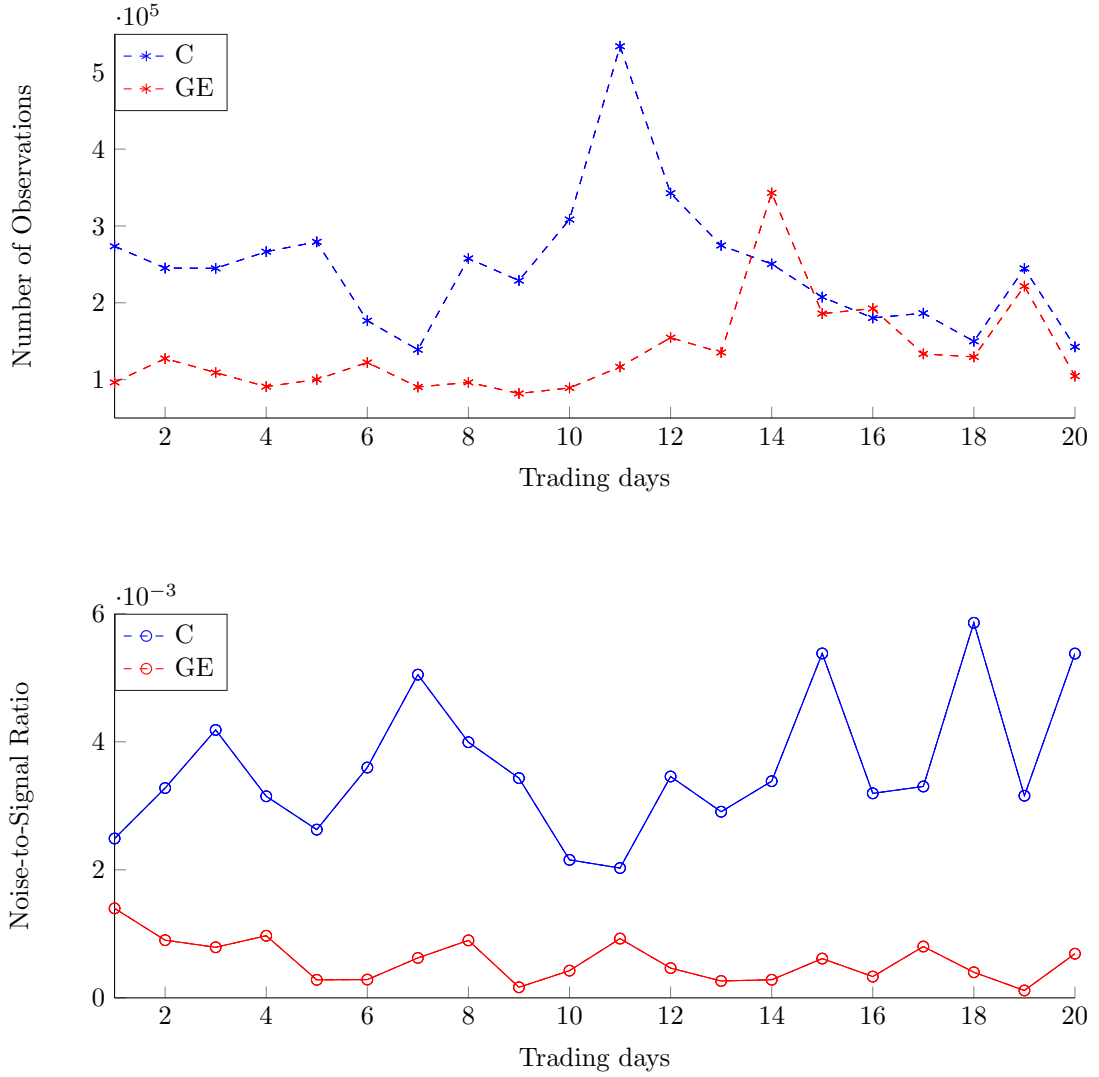


Figure I.1: Number of daily observations of transaction prices (top panel) and noise-to-signal ratio (bottom panel) for Citigroup (C) and General Electric (GE). Sample period: January, 2011, consisting of 20 trading days. In the bottom panel, the noise-to-signal ratio, $\frac{\sigma_U^2}{\int_0^1 \sigma_s^2 ds}$, is estimated by $\frac{\hat{\sigma}_{U,\text{step2}}^2}{\widehat{IV}_{\text{step2}}}$, where $\hat{\sigma}_{U,\text{step2}}^2$ and $\widehat{IV}_{\text{step2}}$ are defined in (32) and (33), respectively. We set $j_n = 30$, $i_n = 15$ and $c = 0.2$.

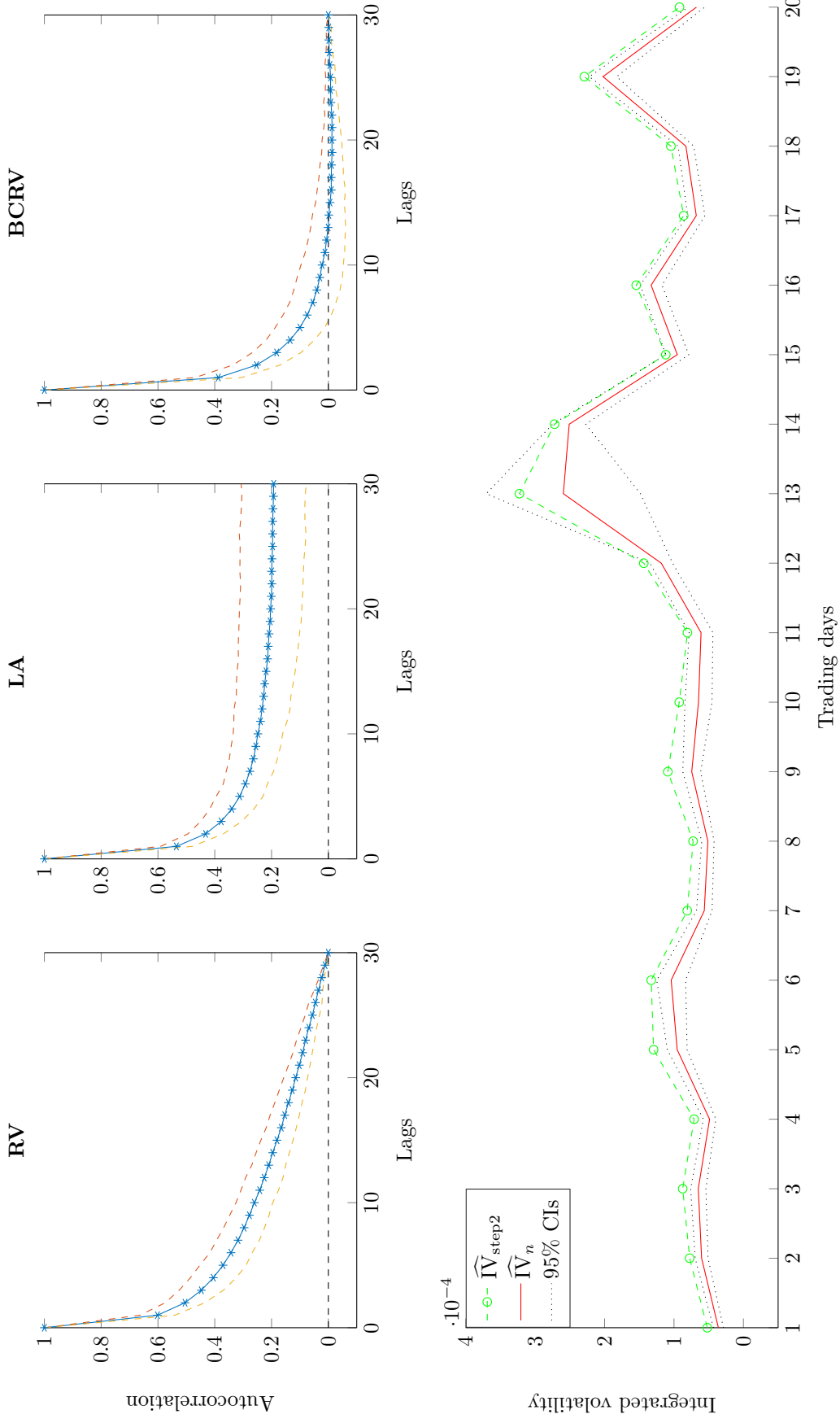


Figure I.2: Autocorrelations of noise and integrated volatility based on transaction data for General Electric (GE). Sample period: January, 2011, consisting of 20 trading days. On average there are 5.8 observations per second in the sample. Top panel: From the left to the right, we display the realized volatility (RV), local averaging (LA), and the bias corrected realized volatility (BCRV) estimators of the autocorrelations of noise against the number of lags j . The three estimators are applied to and next averaged over each of the 20 trading days. The stars indicate the means of the 20 estimates. The dashed lines are 2 standard deviations away from the mean. Bottom panel: Estimation of the integrated volatility. The estimators $\widehat{IV}_{\text{step2}}$ and \widehat{IV}_n are given by (33) and (23). The asymptotic confidence intervals (CIs) are based on the limit distribution in Theorem 4.2. We set $j_n = 30$, $i_n = 15$ and $c = 0.2$.